© 2021. Published by The Company of Biologists Ltd | Journal of Cell Science (2021) 134, jcs236497. doi:10.1242/jcs.236497

RESEARCH ARTICLE

A putative stem-loop structure in *Drosophila crumbs* is required for mRNA localisation in epithelia and germline cells

Srija Bhagavatula and Elisabeth Knust*

ABSTRACT

Crumbs (Crb) is an evolutionarily conserved transmembrane protein localised to the apical membrane of epithelial cells. Loss or mislocalisation of Crb is often associated with disruption of apicobasal cell polarity. *crb* mRNA is also apically enriched in epithelial cells, and, as shown here, accumulates in the oocyte of developing egg chambers. We narrowed down the localisation element (LE) of *crb* mRNA to 47 nucleotides, which form a putative stem-loop structure that may be recognised by Egalitarian (Egl). Mutations in conserved nucleotides abrogate apical transport. *crb* mRNA enrichment in the oocyte is affected in *egl* mutant egg chambers. A CRISPR-based genomic deletion of the *crb* locus that includes the LE disrupts asymmetric *crb* mRNA localisation in epithelia and prevents its accumulation in the oocyte during early stages of oogenesis, but does not affect Crb protein localisation in embryonic and follicular epithelia. However, flies lacking the LE show ectopic Crb protein expression in the nurse cells. These data suggest an additional role for the *Drosophila* 3′-UTR in regulating translation in a tissue-specific manner.

This article has an associated First Person interview with the first author of the paper.

KEY WORDS: 3′-UTR, *stardust*, Follicle epithelium, Apical, mRNA transport, Oogenesis

INTRODUCTION

Epithelia are composed of highly polarised cells, connected to each other by various cell-cell and cell-matrix junctions. Epithelial cell polarity is manifested by the uneven distribution of proteins in the plasma membrane and the underlying cytocortex, resulting in the formation of distinct apical and basolateral domains, with the apical side facing the outside environment or a lumen. In addition, actin filaments and microtubules (MT) are often oriented in a polarised way. This polarised organisation of epithelial cells is instrumental for their function, including their role as barriers to separate the inside from the outside, and their function in secretion, resorption and sensory reception (Macara et al., 2014; Rodriguez-Boulan and Macara, 2014).

Besides proteins, many mRNAs also show a polarised distribution. Several important functions of mRNA localisation have been discovered using various polarised cell types, including epithelial cells, egg cells, neurons or migrating cells. These functions include (1) generating cell types with distinct fates upon cell division by uneven segregation of mRNAs to just one daughter cell (and eventually the proteins encoded by them); (2) concentrating a protein to its site of action by spatially delimited translation of the localised mRNA; (3) preventing ectopic translation and hence deleterious functions of a protein; and (4) facilitating the formation of functional protein assemblies by coordinated spatially restricted translation of localised mRNAs of members of the same multiprotein complex (reviewed by Barr et al., 2016; Cody et al., 2013; Hughes and Simmonds, 2019; Medioni et al., 2012; Parton et al., 2014; Ryder and Lerit, 2018).

RNA localisation within a cell depends on both cis- and trans-acting factors. The RNA itself carries one or several *cis*-acting localisation elements (LEs), also known as the 'zipcode' sequences, mostly found in the 3′-untranslated region (UTR). LEs can exert distinct functions, mediated by binding different proteins (Bullock et al., 2010; reviewed by Barrett et al., 2012; Hamilton and Davis, 2011; Schroeder, 2018). Interactions of LEs with RNA-binding proteins (RBPs) drives ribonucleoprotein (RNP) formation, which is required for mRNA transport or its stabilisation at the final destination (reviewed by Lazzaretti and Bono, 2017; Mayr, 2017; Weis et al., 2013). RNP complexes contain a myriad of translational regulators and adaptor proteins. Some of them, such as the *Drosophila* RBP Egalitarian (Egl), together with the adaptor Bicaudal D (BicD) and the Dynactin protein complex, hook RNP complexes to the minus end-directed motor protein dynein, allowing the localisation of mRNAs at a specific site in the cell by active transport along polarised MTs (Dienstbier et al., 2009; Goldman et al., 2019). The machinery involved in these transport processes are conserved across cell-types (Bullock and Ish-Horowicz, 2001). Translational regulators within the complex ensure that the mRNA is repressed en route and activated only upon receiving appropriate signals at the destination (Chartrand et al., 1999; Gavis and Lehmann, 1994). Often, LEs also serve as translational control due to their overlap with repressor or activator elements (Crucs et al., 2000). Multiple LEs can act synergistically or redundantly in regulating these processes within the cell (Gavis et al., 1996; Kim-Ha et al., 1995; Macdonald et al., 1993; reviewed by Lasko, 2011).

Systematic screens for localised RNA in *Drosophila* performed by *in situ* hybridisation and biochemical approaches have revealed a surprisingly high number of genes, the transcripts of which are localised not only in the early embryo but also at later stages of development and during oogenesis. This behaviour not only applies for coding RNAs, but also for many non-coding RNAs. In several cases, RNA and protein localisation are tightly correlated, and often RNA localisation is required for the proper function of the protein (Barr et al., 2016; Bouvrette et al., 2018; Jambor et al., 2015; Lécuyer et al., 2007; Wilk et al., 2016).

One of the first identified apically localised *Drosophila* mRNAs in epithelia is the mRNA encoded by the gene *crumbs* (*crb*) (Knust et al., 1987). *crb* encodes type I transmembrane proteins, which are restricted to the apical membrane of most epithelia, including

Max-Planck Institute for Molecular Cell Biology and Genetics, 01307 Dresden, Germany.

*Author for correspondence (knust@mpi-cbg.de)

E.K., 0000-0002-2732-9135

Handling Editor: David Glover
Received 12 July 2019; Accepted 30 November 2020

Journal of Cell Science (2021) 134, jcs236497. doi:10.1242/jcs.236497

embryonic and follicular epithelia. In these epithelia, Crb is required for the maintenance of apicobasal polarity and epithelial tissue integrity (Fletcher et al., 2012; Grawe et al., 1996; Sherrard and Fehon, 2015; Tanentzapf et al., 2000; Tepass, 1996; Tepass and Knust, 1990; Tepass et al., 1990). Crb forms membrane-associated multiprotein complexes in the subapical region of epithelial cells, just apical to the zonula adherens (ZA), an adhesion belt encircling the apex of the cell. The Crb complex contains, besides Crb itself, the scaffolding proteins Stardust (Sdt), *Drosophila* PATJ (protein associated with tight junctions) and *D*Lin-7 (also known as Veli), which together define the core Crb complex. The constituents of this complex and their respective interactions are highly conserved from flies to mammals (reviewed by Bulgakova and Knust, 2009; Flores-Benitez and Knust, 2016; Le Bivic, 2013; Tepass, 2012).

Not only the *crb* mRNA, but also the *sdt* mRNA localises apically in *Drosophila* embryonic and follicular epithelial cells (Bachmann et al., 2001; Horne-Badovinac, 2008). Apical delivery of both *crb* and *sdt* mRNAs have been shown to depend on dynein-mediated transport in embryonic and follicular epithelia, mediated by the 3′UTR and an alternatively spliced coding exon, respectively (Horne-Badovinac, 2008; Li et al., 2008). Using overexpression approaches, the authors concluded that apical localisation of *crb* and *sdt* mRNA is essential for apicobasal polarity of the respective epithelia. However, a transgenic fly line, in which the complete endogenous *crb* 3′UTR was replaced by the Simian Virus 40 (SV40)-3′UTR, was reported to be viable and fertile. Crb protein in these animals was still apically localised in the epidermis of stage 11 embryos and in the follicular epithelium of an undefined stage, but data on mRNA localisation were not presented (Cao et al., 2017). The different conclusions on the role of mRNA localisation for protein localisation may be due to different experimental approaches.

Here, we re-evaluated the question on the regulation and significance of *crb* mRNA localisation in epithelia of *Drosophila*. Given that all previous data were based on the removal of the entire 3′UTR (662 nucleotides), we first aimed to determine more precisely the site of the LE within the 3′UTR. We could pinpoint the LE to a stretch of 47 nucleotides, which is predicted to form a stem-loop structure. This structure defines it as a likely recognition site of Egl, which, together with BicD, is required for mRNA transport by cytoplasmic dynein, a minus end-directed MT motor (Dienstbier et al., 2009). Flies carrying a small deletion in the *crb* 3′UTR, which includes the LE, are viable and fertile. Apical *crb* mRNA localisation is abolished in LE-deleted blastodermal and post-blastodermal embryonic epithelia without affecting Crb protein localisation. We further show for the first time that *crb* mRNA is enriched in the oocyte during early stages of oogenesis. Sequences containing the LE are required for MT-dependent transport of *crb* mRNA from the nurse cells to the oocyte, and prevent premature translation of Crb in nurse cells during early stages of oogenesis.

RESULTS

crb mRNA is asymmetrically localised during embryogenesis and oogenesis

It has been previously shown that both the mRNA and the protein encoded by *Drosophila crumbs* (*crb*) are apically localised in many epithelia (Tepass et al., 1990). During embryogenesis, *crb* mRNA shows apical localisation as early as stage 5 during nuclear cycle 13 in the syncytial embryo. This localisation persists throughout the process of cellularisation and is retained in the ectoderm during gastrulation (Fig. 1A-D). Most of the *crb* mRNA form clusters in the cell. This is consistent with earlier observations and has been suggested to be a feature of mRNAs coding for plasma membrane and signalling pathway components (Lécuyer et al., 2007). From stage 9 onward, the apical enrichment of *crb* mRNA is less prominent than in the earlier stages (Fig. 1E). Apical *crb* mRNA can also be detected in the tracheal primordia from stage 11 onwards and in the embryonic hindgut (Fig. 1F-G).

crb mRNA and Crb protein are also apically localised in the follicular epithelium (Horne-Badovinac, 2008; Li et al., 2008; Tanentzapf et al., 2000). We could confirm a clear apical enrichment of *crb* mRNA in the follicular epithelium, but only during stages 10B and 11, not at earlier stages (Fig. 1L-N′). This localisation coincides with the enrichment of apical Crb protein on the entire apical plasma membrane (Sherrard and Fehon, 2015). We additionally detected *crb* mRNA enriched in the oocyte from stage 4 to stage 8, but not at later stages. Until stage 7, *crb* mRNA is predominantly enriched at the posterior pole of the oocyte (Fig. 1H-J), and some *crb* mRNA is detected at the anterior end at stage 8 (Fig. 1K). This behaviour correlates with the orientation of the MT minus ends, which point towards the posterior until stage 7, and towards the anterior after that stage owing to their repolarisation (Theurkauf et al., 1992). Crb protein was clearly detected in the oocyte membrane from stage 9 until stage 12 (Fig. 1O,O′). We cannot exclude localisation of Crb in the oocyte membrane at earlier stages as the oocyte membrane is in very close proximity to the apical membrane of follicle cells before stage 9, and could therefore not be resolved by immunostaining. The presence of *crb* mRNA and Crb protein in the oocyte is consistent with their presence in unfertilised eggs described previously (Laprise et al., 2006).

A stretch of 47 nucleotides of the *crb* 3′UTR are necessary and sufficient for apical mRNA localisation

It has been reported that the *crb* 3′UTR (662 nucleotides) is necessary and sufficient to mediate apical localisation of a transcript injected into the syncytial blastoderm, or when overexpressed in the follicular epithelium using the Gal4/UAS system (Li et al., 2008). To further restrict the region of the 3′UTR of *crb* mRNA essential for its apical localisation, we used the same RNA injection assay (Li et al., 2008; Simmonds et al., 2001; Wilkie, 2001). *In vitro* transcribed Cy-3-labelled RNA, containing the GFP coding sequence, followed by full-length *crb* 3′UTR and an SV40 polyadenylation signal (Fig. 2A, construct 1), was injected into the dorsal side of *Drosophila* syncytial blastoderm. The RNA was injected basal to the nuclei and RNA dynamics was followed using live imaging. RNAs comprising the complete *crb* 3′UTR were rapidly transported apically and localised there within 5 min after injection (Fig. 2B). In contrast, RNAs lacking *crb* 3′ UTR and carrying just the SV40 polyadenylation sequence (del[68-606] *crb* 3′UTR; numbering starts with the first nucleotide after the stop codon) failed to localise even after 10 min (Fig. 2C; Movie 1), confirming previously published results (Li et al., 2008).

In order to narrow down the LE, various truncated versions of the *crb* 3′UTR were sandwiched between the GFP coding sequence and the SV40 polyadenylation sequence (Fig. 2A). mRNA encoded by deletion construct del[68-392] *crb* 3′UTR (construct 3) was properly localised apically (Fig. 2D). In contrast, mRNA encoded by the deletion construct del[392-538] *crb* 3′UTR (construct 4) was ubiquitously distributed (Fig. 2E), suggesting that the deleted region includes an LE necessary to direct the RNA apically. However, RNA containing just this portion of the *crb* 3′UTR ([392-538] *crb* 3′UTR) (construct 5) does not localise apically, suggesting that this region is not sufficient for RNA localisation (Fig. 2F). In contrast, an RNA containing this region plus adjacent sequences ([392-662]

Journal of Cell Science (2021) 134, jcs236497. doi:10.1242/jcs.236497

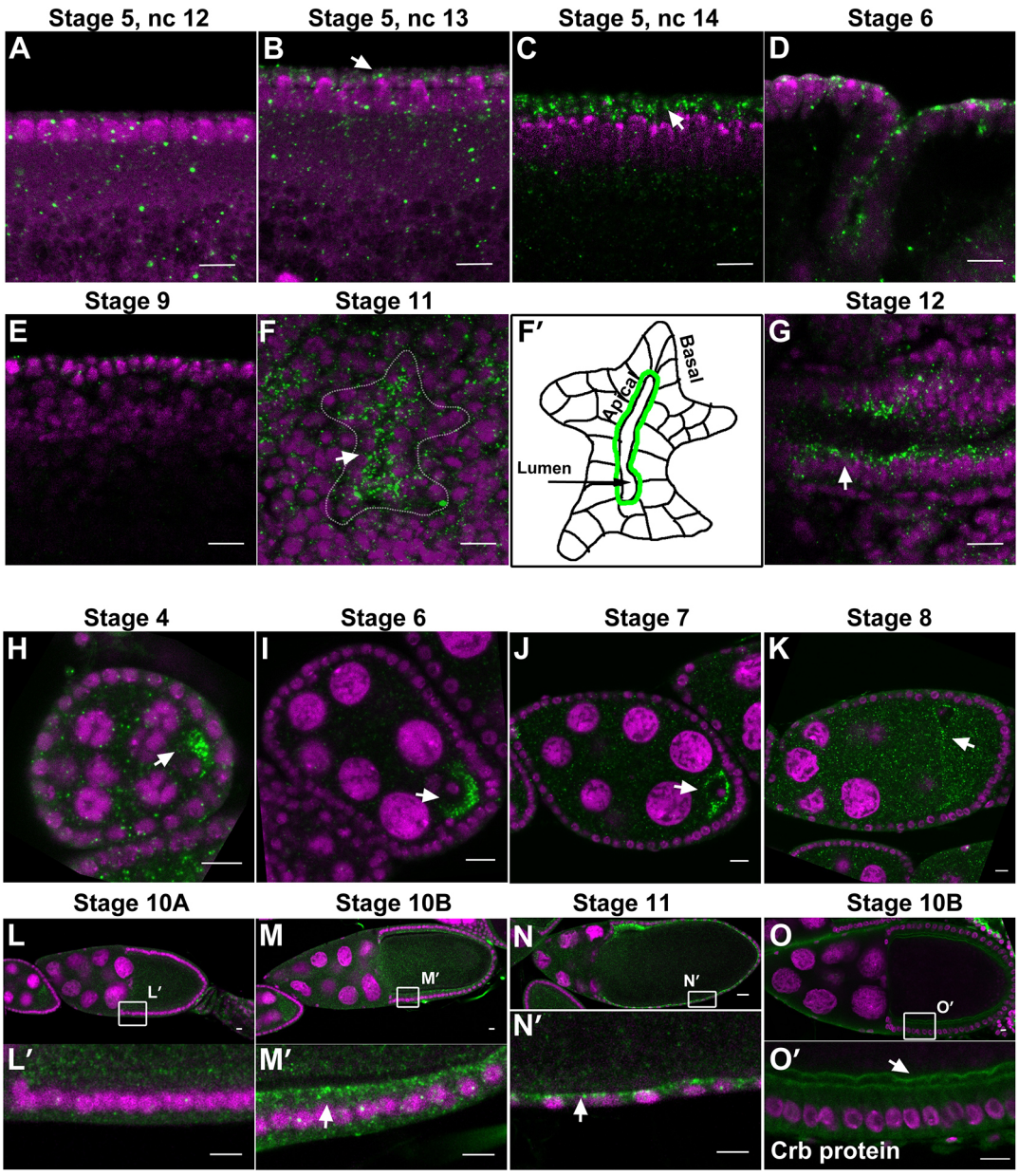

Fig. 1. *crb* mRNA is localised during embryogenesis and oogenesis. (A) *crb* mRNA showed no specific localisation in the syncytial blastoderm at nuclear cycle 12 (nc 12). (B,C) Apical enrichment of *crb* mRNA was evident from nc 13 onwards (B) and most distinct in nc 14 (C) (white arrows). (D,E) During gastrulation and post-gastrulation apical enrichment of *crb* mRNA persists, albeit with reduced signal. (F,F′) *crb* mRNA was apically enriched (white arrow) in cells of the tracheal placode (outlined by the dotted line) during stage 11, as elucidated in the cartoon (F′). (G) The hindgut at stage 12 shows apically enriched *crb* mRNA (white arrow). (H-K) *crb* mRNA was enriched in the oocyte (white arrows) from stages 4 to 8. (L-N′) *crb* mRNA gradually became apically localised (white arrows) in the follicular epithelium during stages 10 and 11. L′, M′ and N′ show higher magnification of the boxed regions in L, M and N, respectively. (O,O′) Crb protein localised in the oocyte membrane (white arrow in O′) during stage 10. Magenta, nuclei; green, *crb* mRNA (H-N′) or Crb protein (O,O′). The presence of *crb* foci in some of the nuclei was not consistent in A-N′. Scale bars: 10 µm.

crb 3′UTR) (construct 6) was apically localised (Fig. 2G; Movie 2). From this, we conclude that the LE of the *crb* mRNA is present in the last 270 nucleotides of its 3′UTR in the region from nucleotide 392 to 662.

To determine the minimal sequence sufficient to localise *crb* mRNA apically, we systematically deleted smaller regions between the 392-662 nucleotides. Deletions removed approximately 50 nucleotides and overlapped with neighbouring deletions by about 25 nucleotides (Fig. 3A). RNAs transcribed from deletion constructs 1 to 3 and 8 localised apically, similar to the full-length *crb* 3′UTR (Fig. 3B; Fig. S1A,B,F), while RNAs transcribed from constructs 4 to 7 failed to localise apically (Fig. 3C; Fig. S1C-E, Movie 3), suggesting that the region common to the four deletions contains the zipcode. The following analysis narrowed down the localisation element to 73 nucleotides covering the nucleotides from 492-565 of the *crb* 3′UTR (Fig. 3A). We further restricted the minimal LE to 47 nucleotides (from 499 to 545; Fig. 3A, construct 9), which is necessary and sufficient for apical mRNA localisation (Fig. 3D; Movie 4). These results allowed us to conclude that the region from 499-545 nucleotides within *crb* 3′UTR constitutes the zipcode that determines apical localisation of *crb* mRNA in the syncytial blastoderm.

Journal of Cell Science (2021) 134, jcs236497. doi:10.1242/jcs.236497

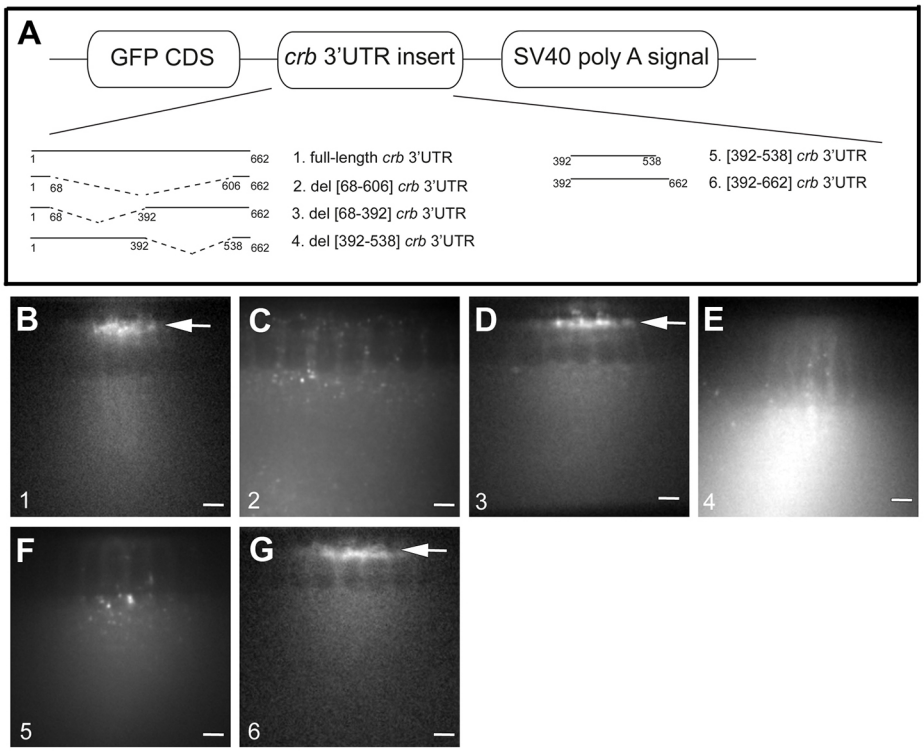

Fig. 2. The region between nucleotides 392-662 of the *crb* 3′UTR contains the mRNA LE. (A) Schematic of the six constructs used as template for mRNA synthesis. The respective sequences of the *crb* 3′UTR are inserted between the GFP coding sequence (CDS) and the SV40 polyadenylation signal. (B-G) Cy-3-labelled RNA synthesised from constructs 1-6 (numbering corresponds to that in A) after injection into the syncytial blastoderm. Only RNAs containing the region from 392-662 rapidly localised apically (white arrows in B, D, G). n>10 embryos imaged live for each injection. Scale bars: 10 µm.

Structural features within the 47 bases suggest interaction with Egalitarian

The 47 nucleotides containing the zipcode are highly conserved in different *Drosophila* species (Fig. S2). Given that 3′UTRs in many localised RNAs adopt specific structures, we used the mfold algorithm to predict putative secondary structures in the *crb* 3′UTR (Zuker, 2003). This analysis predicted a stem-loop structure, reminiscent to that of other apically localised mRNAs (Fig. 3E; dos Santos et al., 2008). The stem-loop structure is composed of 18 base pairs, forming a distal and proximal stem, with the proximal stem containing a single base bulge. In addition, the structure contains two loops, one distal loop and one loop separating the two stems. The predicted *crb* LE structure has characteristics of the consensus motifs present within 3′UTRs of RNAs apically transported on MTs by Dynein, BicD and Egl (Bullock and Ish-Horowicz, 2001; Wilkie, 2001), such as that of *wingless* (*wg*), *hairy* (*h*) or *fushi tarazu* (*ftz*) (dos Santos et al., 2008). Similar to these LEs, the two stems in the *crb* LE are UA-rich and sandwiched between CG base pairs (Fig. 3E), considered to confer stability. A UA base pair fourth from the distal loop (light blue in Fig. 3E), shown to be key for localisation in other LEs (dos Santos et al., 2008), is present as well.

In order to confirm the importance of these features within the *crb* LE structure for apical transport, constructs containing mutations in the *crb* LE were transcribed *in vitro* and injected into the *Drosophila* embryo in the same manner as described above. Deletion of one or both CG base pairs (Fig. 3E, orange) resulted in a loss of apical localisation of the RNA (Fig. 3F-H, mutations a, b and c). Deletion of the key UA base pair fourth from the distal loop (light blue in Fig. 3E), as well as deletion of both the UA base pairs close to the proximal bulge (Fig. 3E, black bracket), also resulted in loss of apical localisation (Fig. 3I,J, mutations d and e). However, deletion of only one of the UA bases near the proximal bulge had no effect on mRNA localisation (Fig. 3K, blue bracket, mutation f) (all results summarised in Movie 5). Taken together, these results suggest that formation of the predicted stem-loop structure is likely to be important for *crb* mRNA apical localisation. This raises two questions: (1) what are the trans-acting factors recognising the *crb* LE and the machinery involved in apical transport of the *crb* mRNA?; and (2), is the LE element also required *in vivo* for *crb* mRNA localisation?

Egl and intact MTs are required for proper *crb* mRNA transport in the oocyte

To elucidate the machinery and the trans-acting factors involved in *crb* mRNA transport, we next concentrated on the female germline, a system in which RNA transport has been extensively studied (Weil, 2014). As the conserved features found in the *crb* LE have several features reminiscent of LEs of other mRNAs transported by Egl, we analysed the role of *egl* on *crb* mRNA localisation in egg chambers of mutant females. Egl binds both to the cargo (RNA) and the dynein co-factor BicD, and thus links the mRNA to the dynein-dynactin transport machinery (Dienstbier et al., 2009). In egg chambers of females heterozygous mutant for *egl* (egl^{RC12}/+ or egl^{WU50}/+) *crb* mRNA in the oocyte was strongly reduced (Fig. 4A-C′). In egg chambers of transheterozygous females (egl^{RC12}/egl^{WU50}) the oocyte is not specified (Mach, 1997). In fact, *crb* mRNA in these egg chambers is present ubiquitously throughout the nurse cells (Fig. 4D,D′). The lack of oocyte specification has also been observed upon loss of function of *BicD* (Dienstbier et al., 2009). Therefore, to determine the role of *BicD* in *crb* mRNA transport, we used $BicD^1$, which encodes a constitutively active protein that binds to Dynein independent of the RNA cargo (Cui et al., 2020), and $BicD^2$, shown to behave similar to $BicD^1$ (Larsen et al., 2008; Liu et al., 2013; Vazquez-Pianzola et al., 2014, 2017). *crb* mRNA in $BicD^1$ and $BicD^2$ heterozygous and $BicD^1/BicD^2$ transheterozygous egg chambers appeared to be more tightly localised to the posterior end of the oocyte (Fig. S3).

The majority of mRNA present in the oocyte is synthesised in the nurse cells and transported into the oocyte along MTs by minus-

Journal of Cell Science (2021) 134, jcs236497. doi:10.1242/jcs.236497

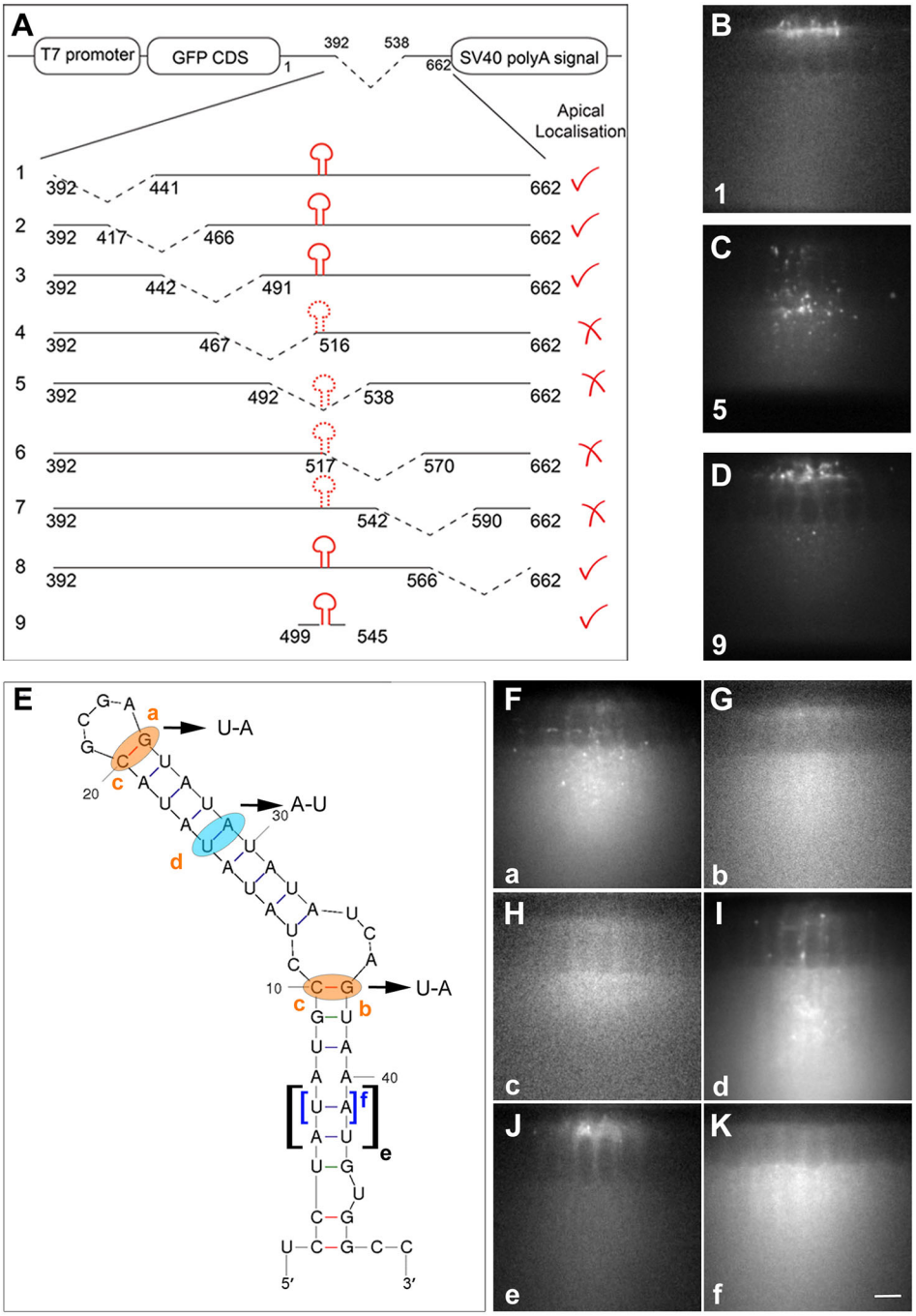

Fig. 3. A stretch of 47 nucleotides within the *crb* 3′UTR are necessary and sufficient for apical *crb* mRNA localisation in the syncytial blastoderm. (A) Schematic of the deletion constructs 1-9 used for mRNA injections. (B-D) Cy-3-labelled RNA synthesised from constructs shown in A after injection into the syncytial blastoderm (numbering corresponds to that in A). A stretch of 47 nucleotides (construct 9) are sufficient for apical mRNA localisation in the syncytial blastoderm (D). (E) Predicted secondary structure of the 47 nucleotides (construct 9 in A). Base pairs highlighted in orange and light blue in the stem-loop structure of the RNA have been mutated: a, C-G replaced by U-A; b, C-G replaced by U-A; c, both C-G pairs (a and b) replaced by U-A pairs; d, U-A base pair replaced by A-U. Base pairs in brackets have been deleted: e, both U-A and A-U base pairs deleted; f, only the U-A base pair deleted. (F-K) Cy-3-labelled RNA synthesised from constructs carrying mutations a to f (labelling shown in E) after injection into the syncytial blastoderm. Only RNA transcribed from construct f localises apically (K). *n*=9 for each injection. Scale bar: 10 µm.

end-directed motor proteins (see, for example, Brendza et al., 2000; Clark et al., 1994; reviewed by Kugler and Lasko, 2009). In addition, Dynein is required to mediate apical localisation of overexpressed *crb* mRNA in the follicular epithelium (Li et al., 2008). This prompted us to analyse the role of MTs in *crb* mRNA transport. Therefore, we fed wild-type females with the MT depolymerising drug colchicine for 12 h before imaging *crb* mRNA in the egg chambers (Fig. 4E-H′). Successful drug treatment was monitored by the mispositioned oocyte nucleus in stage 10 egg chambers (Koch and Spitzer, 1983) (compare Fig. 4G″, G‴ and H″,H‴, white arrowheads). *crb* mRNA enrichment was completely lost in egg chambers of colchicine-treated females, both in the germline (compare Fig. 4E,E′ and F,F′) and in the somatic follicular epithelium (compare Fig. 4G,G′ and H,H′).

crb mRNA is mislocalised *in vivo* upon deletion of the LE

In order to determine the physiological effect of the loss of the LE in the *crb* mRNA, we generated fly lines harbouring deletions in the genomic region encoding the *crb* 3′UTR, using CRISPR/Cas9 technology. We established two fly lines, in which 325 nucleotides (nucleotide 67 to 392) or 193 nucleotides (nucleotide 389 to 582) of the *crb* 3′UTR were deleted, called $crb^{\Delta 325}$ and $crb^{\Delta 193}$, respectively. These deletions were consistent with those described above (Fig. 2A, constructs 3 and 4). Flies carrying either of these deletions were homozygous viable and fertile. Embryos homozygous for $crb^{\Delta 325}$ did not show any defects in apical *crb* mRNA localisation during embryogenesis (Fig. S4). Given the importance of the bases 389 to 582 deleted in $crb^{\Delta 193}$ for mRNA localisation (see Fig. 2E), we performed all further analyses with

Journal of Cell Science (2021) 134, jcs236497. doi:10.1242/jcs.236497

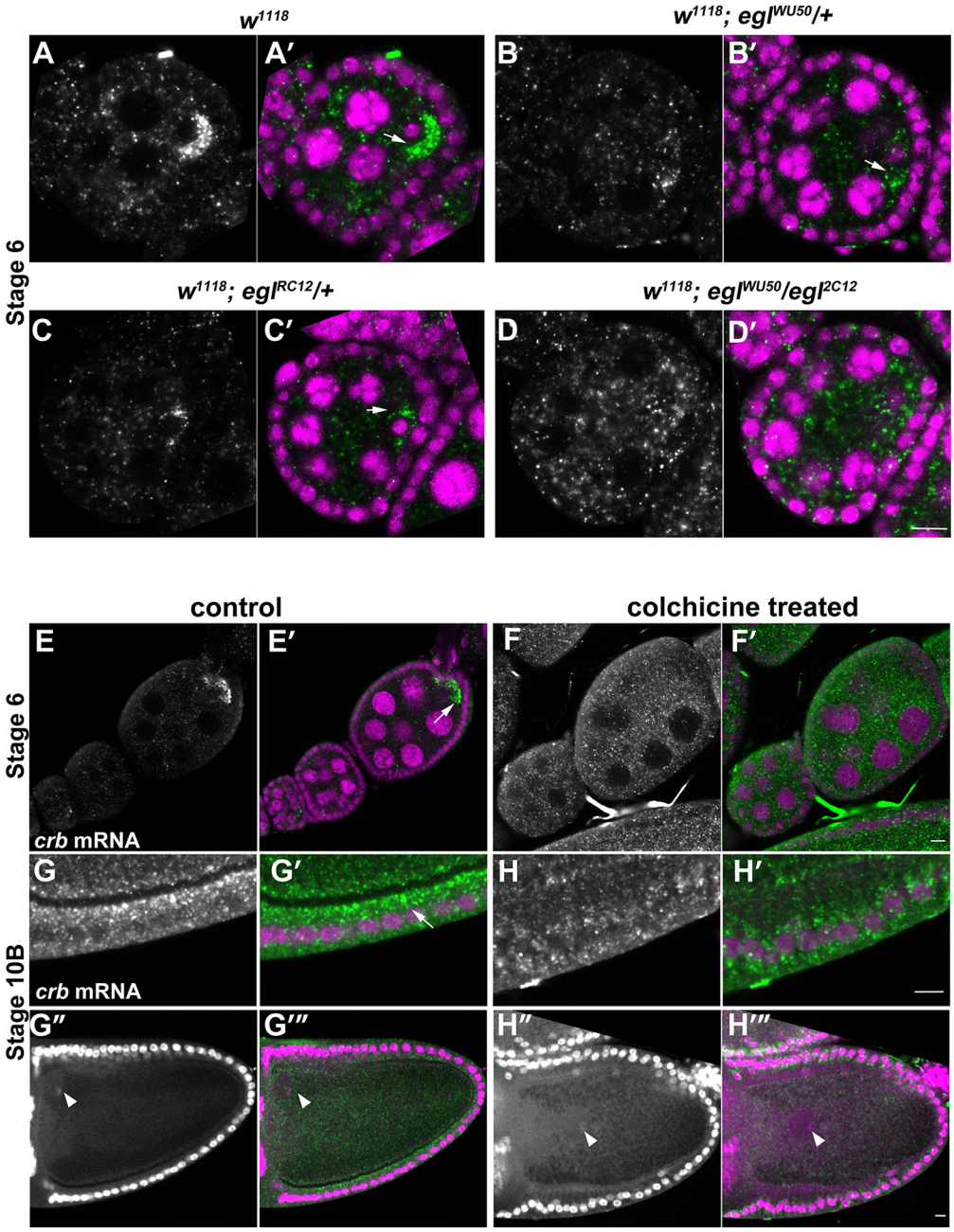

Fig. 4. *crb* mRNA transport requires functional Egl and intact MTs. (A-C′) *crb* mRNA accumulated posteriorly, in the oocyte of control (A,A′), heterozygous egl^{WU50}/+ (B,B′) and egl^{RC12}/+ (C,C′) stage 5 egg chambers (white arrows). Note the strong reduction of *crb* mRNA in the *egl* heterozygous oocytes. (D,D′) In egl^{WU50}/egl^{RC12} transheterozygous egg chambers, the oocyte at the posterior end was not distinguishable, and no accumulation of *crb* mRNA was observed. *n*=7 number of females. Experiment was repeated three times. (E-H‴) *crb* mRNA distribution in egg chambers of untreated (E,E′,G,G′) and colchicine-treated (F,F′,H,H′) females. *crb* mRNA accumulated in the oocyte (E,E′) of stage 6 egg chambers of untreated females but was evenly distributed in egg chambers of colchicine-treated females (F,F′). *crb* mRNA was apically enriched in the follicular epithelium in stage 10B egg chambers of untreated females (G,G′; white arrow) but was evenly distributed in the epithelium after feeding females with colchicine (H,H′). G″-H‴ show overviews of the respective oocytes of the egg chambers. White arrowheads point to the oocyte nucleus, which is mispositioned upon colchicine treatment. *n*=7 number of females. Experiment was repeated two times. Magenta, nuclei; green, *crb* mRNA. Scale bars: 10 µm.

flies carrying this deletion. We generated two lines, namely $crb^{\Delta 193a}$ and $crb^{\Delta 193b}$, by repeated outcrossing of the founder CRISPR mutant line to Oregon R flies to clear the genomic background of unwanted mutations. Both of these lines were analysed in all experiments and shown to behave the same, but in most cases, results from only one line are documented.

Apical mRNA localisation was lost in epithelia of homozygous mutant $crb^{\Delta 193}$ embryos. This was already obvious in the syncytial blastoderm, in which the mRNA was ubiquitously distributed in the cytoplasm in smaller and bigger clusters (Fig. 5A-B′). The image gives the impression that cytoplasmic clusters in the control are smaller. However, careful inspection shows that the bigger clusters are concentrated on the apical side of the nuclei (white arrow in Fig. 5A′). Similarly, *crb* apical mRNA enrichment was abolished in the tracheal placodes of stage 12 embryos (Fig. 5D-E′). However, the total amount of *crb* mRNA as determined by qRT-PCR was not significantly changed, neither at early stages (first 2 h) nor at later stages of embryogenesis (5-10 h) (Fig. 5C,F). In contrast to the mRNA, Crb protein was still restricted to the apical membrane in the tracheal primordium of the mutant (Fig. 5G-H′) and in the epidermis (data not shown), the latter being consistent with previously published data (Cao et al., 2017). Quantitative western blot analyses did not reveal any change in the amount of Crb protein (Fig. 5I-J′). $crb^{\Delta 193}$ mutant females showed normal fecundity and fertility (data not shown), and embryos exhibited normal hatching rates and a wild-type cuticle pattern (Fig. S5A-D). However, we observed that the aspect ratio of eggs laid by $crb^{\Delta 193}$ females was slightly lower than that of control eggs (Fig. S5E-G′).

The presence of *crb* mRNA and Crb protein in the oocyte (see Fig. 1H-K) prompted us to analyse the importance of the LE in *crb*

Journal of Cell Science (2021) 134, jcs236497. doi:10.1242/jcs.236497

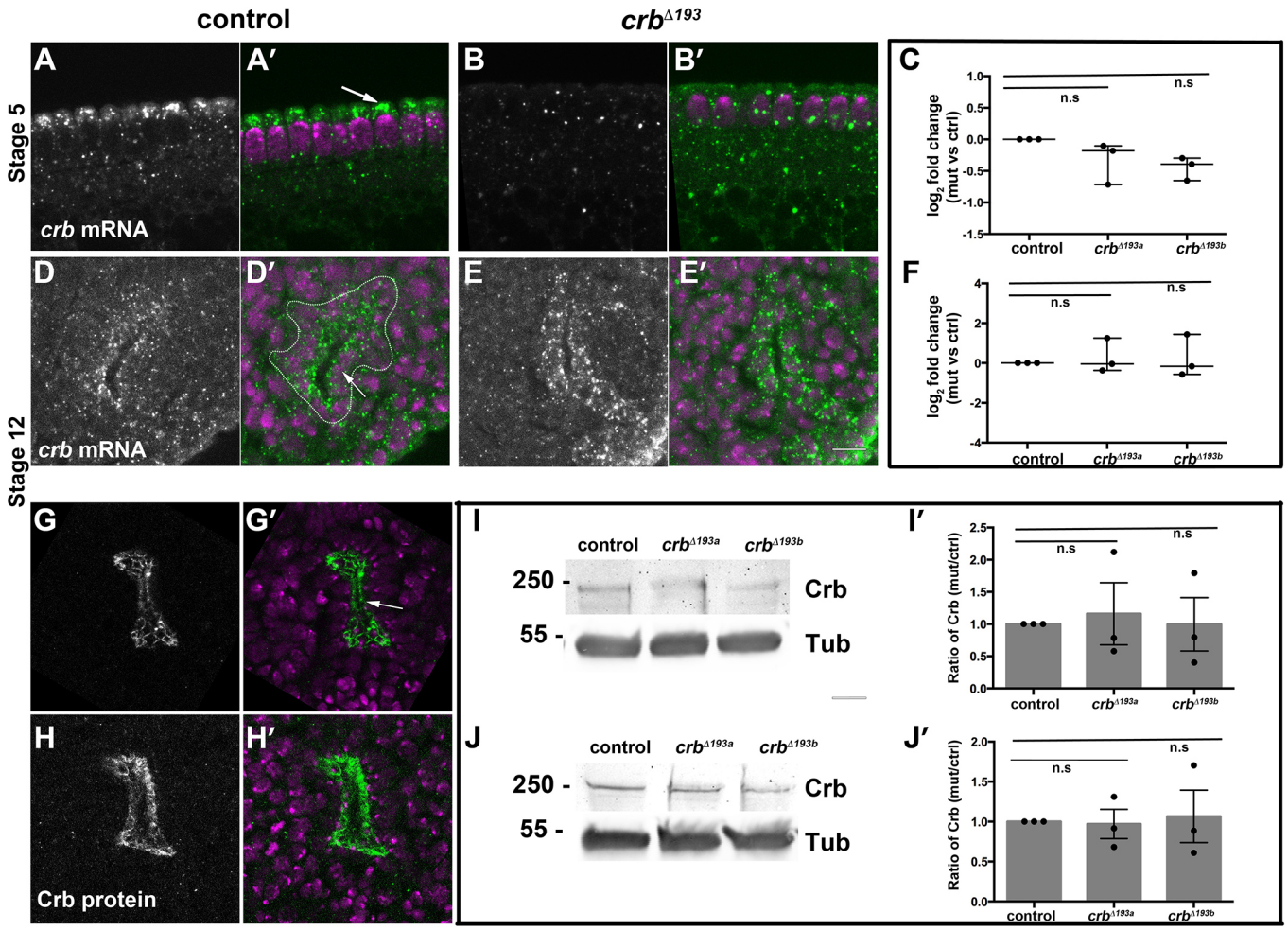

Fig. 5. Crb protein localisation is independent of *crb* mRNA localisation in embryonic epithelia. (A-B′,D-E′) *crb* mRNA was apically localised in the blastoderm of stage 5 embryos (A,A′) and in tracheal cells of stage 12 control embryos (D,D′, white arrows) (white dotted line in D′ outlines the trachael placode). In $crb^{\Delta 193a}$ mutant embryos, apical enrichment of *crb* mRNA was abolished in stage 5 embryos (B,B′) and in the tracheal cells of stage 12 embryos (E,E′). Note that the majority of the bigger clusters seemed to be concentrated on the apical side of the nuclei in the control (white arrow in Fig. 5A′), whereas they were evenly distributed in the mutant. (C,F) Amount of *crb* mRNA was not altered in $crb^{\Delta 193a}$ mutant embryos during the first 2 h of embryogenesis (C) and in overnight collections (F). $P>0.05$, based on a standard paired Student's *t*-test. $n=150$ embryos per sample; $n=3$ for the qRT-PCRs. Error bars represent the interquartile range of the medians. (G-H′) Crb protein was apically localised in tracheal cells of stage 12 control embryos (G,G′; white arrow) and $crb^{\Delta 193a}$ mutant embryos (H,H′). (I-J′) No difference in the amount of Crb protein between control and $crb^{\Delta 193a}$ and $crb^{\Delta 193b}$ mutant embryos was observed in 2-h-old embryos (I,I′) and in overnight collections (J,J′). $n=240$ embryos per sample. $n=3$ for the western blot. Error bars represent s.e.m. *n.s.*, not significant. Magenta, nuclei; green, *crb* mRNA/protein. Scale bar: 10 µm.

3′UTR for mRNA and protein localisation during oogenesis. *crb* mRNA clearly accumulated in the oocyte of wild-type egg chambers at early stages (stage 4 and 7; Fig. 6A,A′,C,C′, white arrow). In contrast, *crb* mRNA was not enriched in the oocyte of $crb^{\Delta 193}$ homozygous mutant egg chambers (Fig. 6B,B′,D,D′). In addition, apical enrichment of *crb* mRNA in the follicular epithelium of stage 10 $crb^{\Delta 193}$ mutant egg chambers was lost (Fig. 6E,E′,F,F′). No defects were found in the total amount of *crb* mRNA in the ovaries as checked by qRT-PCR, suggesting that the stability of the mRNA is not affected by this deletion (Fig. 6G). To conclude, deletion of the LE prevents apical *crb* mRNA localisation in several epithelia and accumulation in the oocyte.

Crb protein is mislocalised during early oogenesis in mutants lacking the LE

mRNA localisation is often required to ensure local protein translation (Lasko, 2012; Medioni et al., 2012; Weil, 2014). Therefore, we next aimed to analyse whether this applies to *crb* as well. Interestingly, $crb^{\Delta 193}$ homozygous egg chambers reveal ectopic Crb protein in the nurse cells, detected in punctate structures at early stages of oogenesis (stage 4-7). These punctae were never observed in wild-type egg chambers in which Crb protein is concentrated in the oocyte (Fig. 6H-K′). However, during later stages, no discernible defects in Crb protein distribution were observed in mutant egg chambers. In the follicular epithelium of $crb^{\Delta 193}$ homozygous mutant egg chambers, the majority of cells revealed apical Crb localisation, similar to wild type (Fig. 6H-M′), despite the fact that the mRNA was not localised. No defect in localisation of apical Sdt, a binding partner of Crb, and of basolateral Discs large 1 (Dlg1) was observed (Fig. S6), suggesting no major aberration in apicobasal polarity. As aberrant mRNA localisation could affect Crb protein translation, we checked the total amount of Crb protein in ovaries of mutant and control females by quantitative western blots. No difference was detected between control and deletion mutants, suggesting that mislocalisation of the mRNA does not affect the translation of the Crb protein in the ovaries (Fig. 6N,N′). To summarise, lack of

Journal of Cell Science (2021) 134, jcs236497. doi:10.1242/jcs.236497

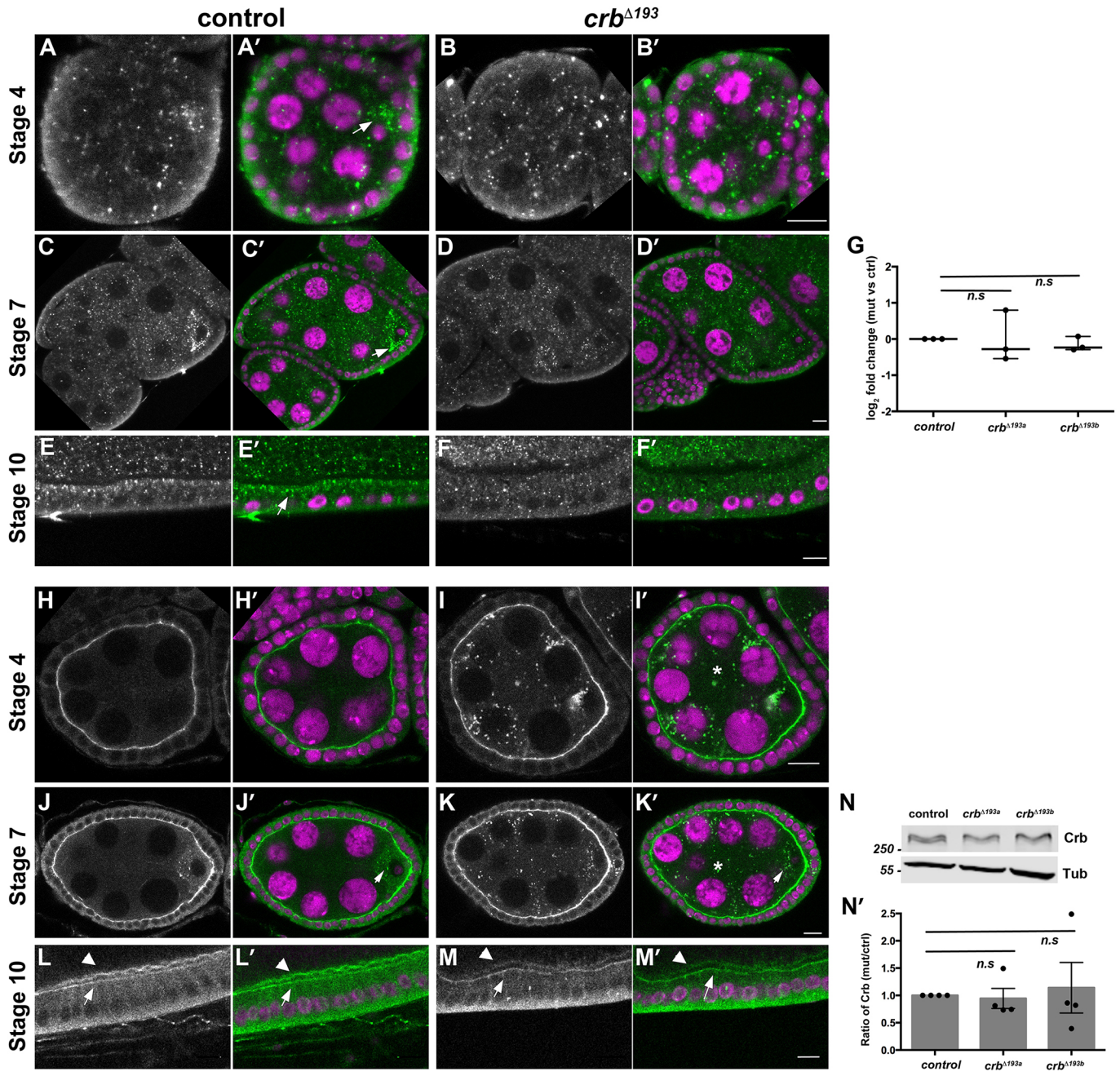

Fig. 6. Loss of the LE impairs *crb* mRNA and protein localisation during oogenesis. (A-F′) *crb* mRNA distribution in control (A,A′,C,C′,E,E′) and $crb^{\Delta 193a}$ mutant (B,B′,D,D′,F,F′) egg chambers. In egg chambers of control females, *crb* mRNA is enriched in the oocyte during early stages (white arrow in A′,C′), and is apically localised in the follicular epithelium of stage 10 (E,E′, white arrow). In egg chambers of $crb^{\Delta 193a}$ mutant females, which lack the LE, *crb* mRNA is no longer enriched in the oocyte (B,B′,D,D′) and is no longer apically localised in the follicle epithelium (F,F′). (G) qRT-PCR with mRNA extracted from whole ovaries showed no difference in the amount of *crb* mRNA between control and $crb^{\Delta 193a}$ and $crb^{\Delta 193b}$ mutants. $P>0.05$, based on standard paired *t*-test. $n=6$ females per sample. Experiment was repeated three times. Error bars represent the interquartile range of the medians. (H-K′) Crb protein was apically localised in the follicular epithelium of both control (H,H′,J,J′) and mutant egg chambers (I,I′,K,K′) during early stages. In germline cells of control egg chambers, Crb protein could only be detected in the oocyte (white arrow), and it is also present in the nurse cells of mutant egg chambers (asterisks) (I,I′,K,K′). (L-M′) Crb protein was apically localised in the plasma membrane of the follicular epithelium (white arrows) and in the plasma membrane of the oocyte (white arrowheads) in both control and $crb^{\Delta 193a}$ mutant egg chambers. $n=7$ females. Experiment was repeated three times. (N,N′) Quantitative western blots from proteins extracted from whole ovaries showed no significant difference in the amount of Crb protein between control and $crb^{\Delta 193a}$ and $crb^{\Delta 193b}$ mutant lines. $P>0.05$, based on standard paired *t*-test. Error bars in N′ indicate s.e.m. $n=5$ females per sample. Experiment was repeated two times. *n.s.*, not significant. Magenta, nuclei; green, *crb* mRNA/protein. Scale bars: 10 µm.

the LE in *crb* 3′UTR affects the accumulation of *crb* mRNA in the oocyte and results in ectopic Crb protein expression in the nurse cells during early stages of oogenesis.

Taken together, data presented here show that Crb protein localisation is independent of *crb* mRNA localisation in the epithelia studied here. Furthermore, the LE in the *crb* 3′UTR is required for proper transport of *crb* mRNA from the nurse cells into the oocyte, a process that requires the function of the Egl-BicD RNP complex and intact MTs. Finally, deletion of the LE of the *crb* 3′ UTR results in ectopic translation of Crb protein in the nurse cells.

Journal of Cell Science (2021) 134, jcs236497. doi:10.1242/jcs.236497

DISCUSSION

The data presented here allow us to draw three main conclusions. First, a stretch of 47 nucleotides in the 3′UTR of the *Drosophila crb* mRNA, which forms a predicted stem-loop structure, possibly recognised by the RBP Egl, is necessary and sufficient to target the mRNA to the apical pole of epithelial cells. Yet, despite the loss of apical *crb* mRNA accumulation in a mutant lacking this sequence, Crb protein is apically localised in embryonic and follicular epithelia. Second, at early stages of oogenesis *crb* mRNA accumulates in the oocyte and Crb protein can be detected in the oocyte plasma membrane from stage 9 onwards. Third, the LE identified in the *crb* 3′UTR is necessary for *crb* mRNA transport from the nurse cells into the oocyte. From these observations, three questions arise: (1) what are the trans-acting factors binding to the LE in the 3′UTR of the *crb* mRNA during oogenesis to control its transport?; (2) what is the function of Crb protein expression in the germline?; and (3) what role does apical *crb* mRNA localisation play in epithelia?

Several trans-acting RBPs have been identified, which exert various functions during oogenesis, including the transport of RNAs from the nurse cells to the oocyte, the repression of premature translation and the anchorage at one of the poles in the oocyte (reviewed by Kato et al., 2012; Lasko, 2012; Weil, 2014). Some RBPs, such as Bruno 1 (Bru1), cover more than one of these functions. Bru1 recognises sequences in the 3′UTR of the *oskar* (*osk*) mRNA and prevents its translation before its arrival at the posterior pole of the oocyte (Kim-Ha et al., 1995). In addition, Bru1 is required for the transport of *osk* mRNA, mediated by several weak signals in the 3′UTR (Ryu et al., 2017). In contrast, Me31B is required for translational repression only, and loss of Me31B causes the premature translation of *osk* and *BicD* mRNAs, but does not affect their transport (Nakamura et al., 2001).

Egl is another protein required for mRNA localisation in the *Drosophila* germline. Egl has been suggested to preferentially bind to LEs containing stem-loop structures identified in several localised transcripts (Dienstbier et al., 2009). Recently, additional Egl-associated mRNAs were identified from extracts of early *Drosophila* embryos by immunoprecipitation of Egl-RNA complexes. Although not among the top candidates, *crb* mRNA was identified in this assay (Vazquez-Pianzola et al., 2017). Our data show that the predicted stem-loop in the *crb* 3′UTR has all the features commonly found in LEs recognised and transported by Egl. And, in fact, mutations in the conserved nucleotides resulted in loss of apical RNA localisation in the syncytial blastoderm. *crb* mRNA enrichment in the oocyte is affected in the germline of *egl* heterozygous females, thus reaffirming the fact that the Egl-mediated machinery involved in mRNA localisation is conserved between embryogenesis and oogenesis (Bullock and Ish-Horowicz, 2001).

Egl mediates RNA transport at multiple levels. Complexed with BicD, Egl links cargo to dynein motors during RNA transport (Dienstbier et al., 2009; Mach, 1997; Navarro et al., 2004; reviewed by Jansen and Niessing, 2012; Vazquez-Pianzola and Suter, 2012). In addition, Egl is required for the organisation of MTs during *Drosophila* oogenesis and for oocyte specification (Mach, 1997), lack of *egl* leads to the absence of a discernible oocyte. Lack of either of these functions could account for the observed ubiquitous *crb* mRNA distribution in mutant egg chambers.

Once mRNA is transported to the minus-ends of the MTs, it must also be anchored at its final destination. In case of anterior localisation of *bicoid* the pool of localised mRNA in the oocyte is maintained by continued transport (Weil et al., 2006). On the other hand, localisation of *osk* mRNA at the posterior pole requires F-actin together with other actin binding proteins (Babu et al., 2004; McNeil et al., 2009; Suyama et al., 2009). *gurken* mRNA localisation depends on an anchor organised by dynein and the hnRNP protein Squid (Delanoue et al., 2007). A similar mechanism anchors *run*, *ftz* and *hb* mRNAs next to the MT-organising centre during early embryogenesis (Delanoue and Davis, 2005). Whether *crb* mRNA also requires mechanisms to anchor it apically in epithelia or posteriorly in the oocyte is not known.

The importance of the stem-loop in the *crb* LE is further underscored by its conservation in all 12 *Drosophila* species for which the genomic sequences have been determined (Drosophila 12 Genomes Consortium et al., 2007). Removal of this stem-loop structure from the *crb* 3′UTR results in the loss of *crb* mRNA localisation *in vivo*, both during oogenesis and embryogenesis. Moreover, ectopic Crb protein expression in the nurse cells of $crb^{\Delta 193}$ mutant egg chambers strongly indicates that in the wild type, Crb protein expression is actively repressed in the nurse cells. We cannot exclude the contribution of sequences other than the LE in transport and/or translational repression, as the *crb* mutant analysed ($crb^{\Delta 193}$) lacks a total of 193 nucleotides. Re-introducing the 47 nucleotides into the genome carrying this deletion would help to answer this question. Furthermore, identifying additional RBP(s) that control *crb* mRNA transport and translational repression would help to elucidate the machinery controlling its transport.

In wild-type egg chambers, *crb* mRNA deposited in the oocyte is translated. So far, we cannot define any function of Crb protein detected in the plasma membrane of the oocyte. We did not find any Crb protein in the plasma membrane of pre-cellularised wild-type embryos, suggesting that Crb protein expression in the oocyte membrane may be transient. However, some *crb* mRNA is stored and transferred to the developing embryo, as both *crb* mRNA and Crb protein can be detected in unfertilised eggs (Laprise et al., 2006).

Unlike results derived from overexpression studies (Li et al., 2008), data presented here show that deleting the LE of the *crb* mRNA does not affect apical localisation of Crb protein in embryonic epithelia and in the follicular epithelium, regardless of the disruption of *crb* mRNA localisation. This is in stark contrast to other examples, in which RNA localisation in epithelia is required for proper protein function. For example, apical localisation of the RNAs encoded by reporters carrying the 3′UTRs of *Drosophila* pair-rule genes, including those from *ftz*, *even skipped* (*eve*) and *h*, ensures the enrichment of the respective reporter proteins in the apical cytocortex (Davis and Ish-Horowicz, 1991). Similarly, impaired apical localisation of RNAs and proteins of pair-rule genes in close proximity to the apically positioned nuclei in blastoderm-stage embryos derived from females with reduced *egl* activity cause segmentation defects in some cases, most likely because of impaired protein localisation upon loss of apical RNA localisation (Bullock et al., 2004). In the case of *unpaired 1* (*upd1*), which encodes a cytokine ligand for the JAK/STAT pathway, apical accumulation of the mRNA in the polar cells of the follicular epithelium is essential for proper secretion of the ligand (Van De Bor et al., 2011).

Interestingly, the follicular epithelium reveals stage-specific distribution of *crb* mRNA, which is apically enriched at stage 10b. This accumulation coincides with a redistribution of Crb protein from the subapical region observed at stage 8 and earlier to the entire apical surface observed from stage 9/10 onwards, a stage characterised by extensive outgrowth of microvilli (Sherrard and Fehon, 2015). Given the observation that increased Crb expression can impact on the size/differentiation of the apical surface of

epithelial cells (Muschalik and Knust, 2011; Pellikka et al., 2002; Wodarz et al., 1995), it is tempting to speculate that apical enrichment of its mRNA may ensure more efficient translation of Crb protein at a stage at which the follicular epithelium undergoes cell shape changes and increases its apical surface area. In mouse intestinal epithelial cells, ribosomes are enriched at the apical pole, and translation efficiency of apically localised mRNAs is ∼twofold higher than that of basally localised RNAs (Moor et al., 2017). As Crb proteins have to traffic through the secretory pathway, it may be interesting to explore whether the apical pole is particularly enriched in endoplasmic reticulum (ER) or Golgi compartments, or harbours a specific ER subtype. Asymmetric ER distribution has recently been shown to precede asymmetric cell division of *Drosophila* neuroblasts (Eritano et al., 2017).

In the epithelia analysed here, lack of *crb* mRNA localisation did not affect Crb protein localisation. However, we cannot exclude that apical transport/enrichment serves other purposes. As both *crb* and *sdt* mRNA are enriched apically in epithelial cells, one may speculate that co-transport of both of them in the same RNPs may ensure efficient translation of the two members of the Crb complex or may serve to recruit other components into the same complex. Complexes containing more than one RNA species, called spreading initiation centres (SICs), have recently been described to occur transiently in mammalian epithelial cells undergoing amoeboid to mesenchymal transition. SICs are enriched in RBPs and poly(A) RNAs to ensure localised translation, which in turn modifies adhesion strength of cells undergoing epithelial to mesenchymal transition (Bergeman et al., 2016). However, we were unable to determine any co-transport of *crb* and *sdt* RNA in the same particle. Preliminary data suggest that fluorescently labelled *sdt* mRNA containing an alternatively spliced exon, exon 3, inserted between the GFP coding region and the SV40-polyadenylation sequence, did not accumulate apically when injected into the syncytium. This exon has been suggested to mediate apical mRNA transport upon overexpression in the follicular epithelium or embryonic salivary glands (Horne-Badovinac, 2008). The discrepancy in our data can be explained either by the different experimental approaches used (overexpression of UAS-transgenes versus injection of labelled RNA), or by the presence of a different LE responsible for apical *sdt* mRNA in the syncytial blastoderm (compared to the follicular epithelium and the salivary gland). In fact, a CRISPR-induced *sdt* allele, in which exon 3 was replaced by GFP, is viable and fertile, and the Sdt protein is localised apically in embryonic epithelia (Perez-Mockus et al., 2017).

Taken together, a LE of 47 nucleotides in the *crb* 3′UTR is required for apical localisation of *crb* mRNA in several epithelia and for proper transport of *crb* mRNA from the nurse cells into the oocyte. Although our studies did not reveal any function of this element for viability, it may be important to confer robustness to the system, perhaps by ensuring a rapid assembly of the Crb protein complex on the apical pole, or for proper differentiation/formation of the apical membrane. In the future, the $crb^{\Delta 193}$ allele characterised here is ideally suited to create a sensitised background, which can, for example, be used to identify additional components involved.

MATERIALS AND METHODS

Fly stocks

Flies were maintained at 25°C with 65% humidity unless otherwise stated. The following fly lines were used: OregonR as wild-type and w^{1118};; as control. To characterise *crb* mRNA localisation in RBP mutants, the alleles egl^{WU50} and egl^{RC12} were used for *egl* and $BicD^{1}$ (also known as $BicD^{7134}$), and $BicD^{2}$ dominant mutations were used for *bicD* (alleles described by Mohler and Wieschaus, 1986; Schüpbach and Wieschaus, 1991). *yw; egl^{WU50} bw sp/SM1*, *egl^{RC12} cn bw/CyO*, *100DTS* and *b $BicD^{7134}$ tud^{1} bw/CyO* were obtained as a kind gift from Dr Anne Ephrussie (European Molecular Biology Laboratory, Developmental Biology Unit, Heidelberg, Germany). The following fly lines were obtained from the Bloomington *Drosophila* Stock Center (BDSC): *$BicD^{2}$ cn^{1} tud^{1} bw^{1}/CyO* (BDSC 3243), *y^{1} P(nos-cas9, w+) M(3xP3-RFP.attP)ZH-2A w** (BDSC 54591) (Port et al., 2014) and *y^{1} M(vas-Cas9)ZH-2A w^{1118}* (Sebo et al., 2014) (BDSC 52669) were used for injections of CRISPR constructs. w^{1118};; $crb^{\Delta 193a}$, w^{1118} ;; $crb^{\Delta 193b}$, and w^{1118};; $crb^{\Delta 325}$ were generated as part of this work. w^{1118};; crb^{GX24}/TM3, twi-GAL4 UAS-EGFP Sb^{1} Ser^{1}; a *crb* null allele from Huang et al. (2009) and *w^{1118}; Df(3R)Exel6199, P{XP-U}Exel6199/TM3, twi-GAL4 UAS-EGFP Sb^{1} Ser^{1}*; (BDSC 7678), a deficiency line, were used as negative controls.

Generation of *crb* alleles by CRISPR/Cas9-mediated genomic deletions

Designing sgRNAs

The *crb* 3′UTR genomic sequence of the C-isoform was chosen from the *Drosophila melanogaster* genome database (genome version r_6, accessed from Flybase: www.flybase.org/). It is longer than that of the other isoforms and includes the complete 3′UTRs of all splice variants. Target sites within the *crb* 3′UTR were picked and oligos for the seed sequence designed using http://targetfinder.flycrispr.neuro.brown.edu/. Prediction parameter was set to choose all CRISPR targets with 5′GG. Primer sequences are listed in Table S1. The stringency was set to maximum according to the software, and the PAM sequences of only NGG triplets were accepted. There were two oligos for each target, complementary to each other. The oligos contained a 5′ phosphoryl group and were ordered from Eurofins. The complementary oligonucleotides were annealed and ligated into the BbsI site of the pCFD3-dU6:3 vector (Addgene, 49410) and transformed into DH5α competent cells and plated on ampicillin plates. Plasmids isolated from individual colonies were sequenced to screen for positives. Plasmid DNA for injections was prepared using the PureLink HiPure Plasmid Miniprep kit (Invitrogen, K210002).

Generation of fly lines with genomic deletions

Flies carrying genomic deletions were obtained by injecting pairs of plasmids encoding sgRNA complementary to the ends of the respective deletion into *nos::Cas9* embryos [BDSC 54591: *y^{1} P(nos-cas9, w+) M(3xP3-RFP.attP)ZH-2A w**]. In these flies, Cas9 expression, driven by the *nanos* promoter, is restricted to the female germline. Plasmids for the del[67-392] *crb* 3′UTR fly line were injected in house, whereas the plasmids for the del[389-582] *crb* 3′UTR fly line were sent to BestGene for injections. Flies obtained from surviving larvae were crossed with each other. The following crossing scheme was modified from Bassett and Liu (2014). F1 males were individually crossed to w^{1118} virgins. After successful mating, DNA of F1 males was sequenced to confirm the presence of the deletion. At least 150 to 200 F1 males were screened. Progenies of F1 males carrying the deletion were further crossed to third chromosome balancer lines. After confirming the deletion in F2 males, F3 males and females were intercrossed and homozygous mutant stocks were established.

Preparation of embryos and ovaries for immunohistochemistry and fluorescent *in situ* hybridisation

Embryos were collected on apple juice agar plates at 25°C unless mentioned otherwise. For mRNA localisation studies throughout embryogenesis, overnight collections of embryos were used. To obtain stage 5 and stage 12 embryos, 1- and 5-h collections were aged for 2 h and 5 h, respectively. Embryos were fixed according to standard protocols. Eggs were dechorionated in 50% bleach for 2 min and fixed in 4% formaldehyde/heptane mixture for 20 min at room temperature. Devitellinisation was performed by rigorous shaking in a 1:1 ratio of methanol and formaldehyde, and the embryos were stored at −20°C in methanol until further processing.

To prepare ovaries, 1-day-old female flies were fed with fresh yeast for 2 days before fixation. Ovaries were dissected in PBS, immediately fixed in 4% paraformaldehyde in PBS for 20 min and rinsed twice in PBS. Samples

were processed for immunohistochemistry. For Fluorescent *In Situ* Hybridisation (FISH), specimens were passed through increasing concentrations of ethanol (in PBS).

FISH

Probes were generated using template plasmids with the pBSK(+) vector backbone containing exon 2 of the *crb* cDNA, cloned between the T7 and T3 RNA polymerase promoters for the generation of anti-sense and sense probes, respectively. Digoxigenin-labelled probes were generated according to the manufacturer's instructions using the DIG RNA labelling mix (Roche, 11277065910) and the respective RNA polymerases. Transcribed RNA was purified using the RNeasy Min-elute Cleanup kit (Qiagen, 74204).

In situ hybridisations essentially followed previous protocols (Jambor et al., 2015; Tomancak et al., 2002). Postfixed embryos and ovaries were incubated in prehybridisation buffer [50% formamide, 20% of 20× SSC (NaCl 3 M and NaCit 300 mM), and 0.01% Tween 20 – volume made up with DEPC-treated water] for 1 h at 57°C. Hybridisations with digoxigenin-labelled RNA probes were performed overnight at 57°C in hybridisation buffer [50% formamide, 20% of 20× SSC, 0.01% Tween 20 and 0.05% dextran sulphate – rest of the volume made up with DEPC-treated water]. Samples were washed four times with washing buffer [50% formamide, 0.1% of 20× SSC and 0.01% Tween 20 – volume made up with DEPC-treated water], and four times in PBS plus 0.1% Tween 20 (PBST) for 30 min each, blocked in 5% normal goat serum in PBST for 1 h and incubated overnight at 4°C with peroxidase-conjugated anti-digoxigenin antibody (1:200; Sigma-Aldrich, 11 207 733 910). Samples were washed eight times in PBST for 20 min each, followed by incubation in a 1:100 dilution of fluorescent tyramide substrate (Perkin Elmer, NEL744001KT) for 1 h. After washing eight times for 20 min each, specimens were mounted in Vectashield mounting medium (Vector Laboratories).

Immunostaining

Embryos

The embryos were washed six times quickly with PBST and then blocked for 2 h with 5% normal horse serum/PBST. The embryos were then incubated overnight at 4°C in primary antibody [rat anti-Crb 2.8 (Richard et al., 2006)], diluted to 1:1000 in blocking solution. The next day, the primary antibody was removed and the embryos were rinsed three times and washed three times for 5 min each with PBST. They were then incubated in secondary antibody [goat anti-rat 567 (Thermo Fisher Scientific, A-11006; diluted 1:1000 in PBST] for 2 h. The embryos were then washed three times with PBST for 10 min each. DAPI was added at a final concentration of 2 µg/ml in the intermediate wash. The embryos were rinsed once in PBS and then mounted in Vectashield mounting medium.

Ovaries

Ovary samples postfixation, were washed three times with PBS plus 0.5% Triton X (PBST-X) for 20 min each. They were blocked with 5% bovine serum albumin /PBST for 1 h, followed by incubation with a primary antibody, diluted in blocking solution, overnight at 4°C. Thereafter, the primary antibody was removed, and the samples were washed with PBST-X three times for 20 min each. Samples were blocked again for 10 min and incubated in a 1:1000 dilution of the appropriate secondary antibody for 2 h at room temperature. Post incubation, samples were again washed three times with PBST-X for 20 min each and then three times with PBS for 5 min each. DAPI was added at a final concentration of 2 µg/ml in one of the washes. Finally, the samples were mounted in Vectashield mounting medium. During mounting, the ovarioles were separated more vigorously with the help of a needle in order to ease the imaging of individual ovarioles and follicles. Primary antibodies used were as follows: guinea pig anti-Crb DE15161/Crb2.8 (1:500) [raised against the same epitope as described in Richard et al. (2006)], rabbit anti-Sdt-C-PDZ (1:1000) (Berger et al., 2007) and mouse anti-Dlg4F3 (1:1000) from the Developmental Studies Hybridoma Bank (DSHB). The antibody 4F3 anti-discs large (https://dshb.biology.uiowa.edu/4F3-anti-discs-large) was deposited in the DSHB by C. Goodman (University of California, Berkeley, USA). All secondary antibodies were used at a dilution of 1:1000: donkey anti-guinea pig IgG Alexa Fluor 568 (Invitrogen, A11075), goat anti-rabbit IgG Alexa Fluor 568 (Invitrogen, A11036) and goat anti-mouse Alexa Fluor 488 (Invitrogen, A11029).

Colchicine treatment

Virgin females were collected, aged for a day at 25°C, starved for 5 h and then fed with yeast containing 65 µg/ml colchicine for 15 h (Januschke, 2006). An equal number of control females were fed with yeast without the drug. Ovaries were immediately isolated from these females, fixed and then processed for FISH and immunohistochemistry.

Cloning of the deletion variants

The *crb* 3′UTR sequence was amplified from the vector pUAST-attB-CD2-MARNKRAT-GFP- *crb*-3′UTR (Kumichel et al., 2015) and cloned into the BamHI restriction sites of the vector pT7-GFP-SV40 [generously provided by K. Kapp, University of Kassel, Germany). As this sequence contained only 568 nucleotides of the *crb* 3′UTR, the remaining sequence, together with the SV40 polyadenylation signal sequence, was added using the New England Bio Labs Gibson assembly protocol for multi-fragment cloning to generate the pT7-GFP-*crb* 3′UTR-SV40 vector, which contains 662 nucleotides of the *crb* 3′UTR.

Sequences of the *crb* 3′UTR with regions deleted between the nucleotide ranges, 193-396, 68-396 and 68-601 were synthesised and cloned into the XbaI site of pUC57 (GenScript). Deletion constructs were cloned into the XbaI site of the pT7-GFP-SV40 vector to obtain pT7-GFP-del[193-396] *crb* 3′UTR-SV40, pT7-GFP-del[68-396] *crb* 3′UTR-SV40 and pT7-GFP-del[68-601] *crb* 3′UTR-SV40. Primers used were 3UTRSV40FP1 and 3UTRSV40RP1 to amplify the insert, and 3UTRFP2 and 3UTRRP2 to amplify the vector (Table S1).

The construct carrying the deletion bases (392-538) of the *crb* 3′UTR was generated using the Stratagene Quikchange II Site Directed Mutagenesis protocol. For this, the vector pT7-GFP-*crb* 3′UTR-SV40 was used as a template and the desired deletion was introduced using the primers del[3-5]FP and del[3-5]RP (Table S1).

The construct [392-538] *crb* 3′UTR was amplified using the primer pair ls_[3-5]FP and ls_[3-5]RP; and the construct [392-646] *crb* 3′UTR was amplified using ls_[3-5]FP and ls_[3-5]RP2 from the vector pT7-GFP-*crb* 3′UTR-SV40. The amplified products were cloned into the XbaI site of the vector pT7-GFP-SV40. The systematic 50 base deletions within the *crb* 3′UTR region [392-662] were performed using site-directed mutagenesis. The primer pairs used for each deletion were as follows: del1_[392-441] *crb* 3′UTR (construct 1), [3-5]delFP1 and [3-5]delRP1; del2_[417-466] *crb* 3′UTR (construct 2), [3-5]delFP2 and [3-5]delRP2; del3_[442-491] *crb* 3′UTR (construct 3), [3-5]delFP3 and [3-5]delRP3; del4_[467-508] *crb* 3′UTR (construct 4), [3-5]delFP4 and [3-5]delRP4; del5_[492-538] *crb* 3′UTR (construct 5), [3-5]delFP5 and [3-5]delRP5; del6_[517-566] *crb* 3′UTR (construct 6), [3-5]delFP6 and [3-5]delRP6; del7_[542-591] *crb* 3′UTR (construct 7), [3-5]delFP7 and [3-5]delRP7; and del8_[567-616] *crb* 3′UTR (construct 8), [3-5]delFP8 and [3-5]delRP8. To generate the rescue construct containing the 47 nucleotide LE, [499-545] *crb* 3′UTR (construct 9), 5′ phosphorylated sense (*crb*LS47_FP) and anti-sense (*crb*LS47_RP) oligonucleotides were synthesised. The oligos, flanked by sticky ends, were annealed together and cloned into the XbaI site of the pT7-GFP-SV40 vector.

Mutations within the *crb* LE in the specific features required by Egl transport were generated using site-directed mutagenesis. The primer pairs used for each mutation were as follows: construct 'a', SLMut1_FP and SLMut1_RP; construct 'b', SLMut3_FP and SLMut3_RP; construct 'c', SLMut2_FPand SLMut2_RP, construct 'd', SLMut4_FP and SLMut4_RP; construct 'e', SLMut5_FP and SLMut5_RP; and construct 'f', SLMut6_FP and SLMut6_RP. Primers used to make each deletion construct are listed in Table S1.

RNA embryo injections and imaging

RNAs injected into the embryos were *in vitro* transcribed from the plasmid templates described above after linearisation with NaeI. ChromaTide Alexa Fluor 546-14-UTP (Thermo Fisher Scientific, C11404) or ChromaTide Alexa Fluor 488-5-UTP Alexa (Thermo Fisher Scientific, C11403) were used for fluorescent labelling of the RNAs, based on the instruction

provided by the manufacturer. *In vitro* transcription was set up as a 20 µl reaction using the T7 RNA polymerase (Roche, 10 881 775 001).

We essentially applied the RNA injection assay described earlier (Li et al., 2008; Simmonds et al., 2001; Wilkie, 2001). One-hour egg collections of wild-type embryos, fixed on a double-sided tape, were dechorionated manually, and were transferred to a Petri dish with a cover slip bottom and held in place with heptane glue. Halocarbon oil 10S (VWR, VWRC24627.188) was added to cover the embryos. Injections were performed using a mechanised needle holder connected to a Femtojet Eppendorf injection setup. An Olympus IX71 spinning disc confocal microscope equipped with an iXon detector was used to image the embryos. Embryos that started cellularisation were injected with a final concentration of 250 ng/µl RNA. A 60× solid immersion lens objective with a numerical aperture of 1.3 was used for injections and imaging. Embryos were imaged immediately after injection with a laser excitation at 567 nm. Movies were taken for up to 10 min for the control injections, in which the RNA was localised within 5 min after injection. For RNAs that did not show apical enrichment, movies were acquired for up to 20 min in order to account for delayed enrichment. The exposure time used was 600 ms with a frame rate of 0.5 frames/sec. The acquired images were analysed using Fiji Image analysis software (Schindelin et al., 2012). At least 15 embryos were injected for each of the transcripts. The images and supplementary movies featured in this study have been smoothened using the Gaussian blur with a sigma value of 0.5.

Imaging and image analysis

All samples post immunostaining and FISH were imaged with an LSM 880 Laser Scanning Confocal Microscope (Carl Zeiss), using the 20×/0.8 air objective and the Zeiss 63×/1.2 multi-immersion objective. The generation of *z*-stacks was achieved using a section interval of 1.5 or 2 µm taken through the mounted tissues. All images shown here are single optical sections. Images were analysed using Fiji (Schindelin et al., 2012) and processed using Photoshop.

Evaluation of fecundity, fertility, embryonic lethality and cuticle preparation

Same-aged females (15 animals) of the genotypes to be analysed were crossed to $crb^{\Delta 193}$ males at 18°C and 25°C in regular culture vials. Flies were transferred from vials to embryo collection cages after 2 days. Three such cages were set up for each genotype at both temperatures. To calculate fecundity/female/hour, the number of eggs laid was counted for each genotype and divided by the number of females alive in the cage, and the period of egg lay (24 h for 18°C and 12 h for 25°C). Of the total number of eggs laid, the number of eggs hatched per female was calculated to determine fertility/female for both temperatures.

w^{1118} and $crb^{\Delta 193}$ females were crossed to males of respective genotypes in normal culture vials and transferred to embryo collection cages after 2 to 3 days. The required genotypes of the embryos were selected (based on fluorescent markers) and analysed. The genotypes were as follows: (a) w^{1118};;, (b) w^{1118};;$crb^{\Delta 193}$, (c) w^{1118};; +/$crb^{\Delta 193}$, (d) w^{1118};;+/crb^{GX24} w^{+}, (e) w^{1118};; $crb^{\Delta 193}$/crb^{GX24},w^{+}, (f) w^{1118};;+/Df6199, w^{+mC}, and (g) w^{1118};; $crb^{\Delta 193}$/Df6199,w^{+mC}. Embryonic lethality for each genotype was calculated as the fraction of embryos hatched out of those laid. Cuticles of fully differentiated embryos were essentially prepared according to the method described by Wieschaus and Nüsslein-Volhard (1986).

qRT-PCR

For RNA extraction, embryos and dissected ovaries were homogenised in 1 ml of TRIzol (Invitrogen) and, after addition of 200 µl chloroform, mixed vigorously and incubated on ice for 10 min. Homogenates were centrifuged for 15 min at 12,000 ***g*** and 4°C, and the upper clear phase was collected. After adding 500 µl isopropanol, samples were centrifuged for 10 min at 12,000 ***g*** and 4°C to precipitate the RNA. The supernatant was then removed. The RNA pellet was washed with 1 ml of 75% ethanol and centrifuged as above. RNA pellets were air-dried and dissolved in 20 µl nuclease-free water. RNA quality was checked using Bioanalyzer testing.

cDNA was synthesised using 1 µg of total RNA: a 20 µl reaction volume was set up by mixing 1 µl random primers (50 ng/µl), 1 µl dNTP mix (10 mM), 2 µl 10× buffer, 4 µl $MgCl_2$ (25 mM), 2 µl DTT (0.1 M), 1 µl RNAseOUT Ribonuclease Inhibitor (Invitrogen, 10777019) and 1 µl Superscript II Reverse Transcriptase (Invitrogen, 18064014) according to the manufacturer's instructions. The reaction mixture was incubated at room temperature for 10 min, followed by an incubation at 42°C for 50 min and heat inactivation of the enzyme at 70°C for 15 min.

qRT-PCR reactions were set up in triplicates for all samples. The reaction mixture contained template cDNA (20–50 ng), Pan-Crb forward primer [0.4 µl (stock 10 µM)], Pan-Crb reverse primer [0.4 µl (stock 10 µM)] (Sarita Hebbar and Julia Jarrells; MPI-CBG Dresden, Germany) and SYBR Green (Invitrogen). The following cycling conditions were applied: 15 min at 95°C, 40 cycles at 98°C for 20 s each, 55°C for 20 s, 72°C for 20 s, and a final elongation at 72°C for 10 min. As a control, Gapdh primers were used under the same reaction conditions (see Table S1 for primer sequences).

Western blotting

Embryos and dissected ovaries were crushed in 90 µl of radioimmunoprecipitation lysis buffer containing 130 mM NaCl, 50 mM Tris-HCl, pH 8.0, 0.5% Triton X-100 and protease inhibitor (Roche, 4693159001). After incubation on ice for 30 min, 30 µl 4× SDS sample buffer was added to the homogenate and samples were incubated for 15 min at 65°C. Proteins were separated by SDS-PAGE and blotted onto nitrocellulose 0.45 membranes (Amersham). The membrane was blocked in 5% skimmed milk followed by overnight incubation at 4°C with primary antibodies. Rat anti-Crb 2.8 antibody (Richard et al., 2006) was diluted 1:1000 in blocking buffer and mouse anti-Tubulin antibody (Sigma-Aldrich) was diluted 1:5000 in blocking buffer. Blots were washed thoroughly and incubated in fluorescently labelled goat anti-mouse 488 (Invitrogen, A-21235) and goat anti-rat IgG Alexa Fluor 647 (Invitrogen, A-21247) secondary antibodies (1:10,000), and bands were visualised using an Illumina machine.

Acknowledgements

We thank the BDSC for fly stocks and the DSHB for antibodies. This work was supported by the fly facility, the light microscopy facility and the sequencing facility of the Max-Planck Institute of Molecular Cell Biology. Specials thanks go to all lab members, in particular David Flores-Benitez for advice on experiments and constructive input, and Helena Klara Jambor and Shovamayee Maharana for helpful discussions. We thank Sarah Behrens and Catrin Hälsig for technical support; Pavel Mejstrik for technical advice; and the fly keepers Sven Ssykor, Cornelia Mass and Stefan Wernicke for the excellent care of our flies.

Competing interests

The authors declare no competing or financial interests.

Author contributions

Conceptualization: S.B., E.K.; Methodology: S.B.; Validation: S.B.; Formal analysis: S.B.; Investigation: S.B.; Resources: E.K.; Data curation: S.B.; Writing - original draft: S.B.; Writing - review & editing: S.B., E.K.; Visualization: S.B.; Supervision: E.K.; Project administration: E.K.; Funding acquisition: E.K.

Funding

This work was funded by the Max-Planck-Gesellschaft.

Supplementary information

Supplementary information available online at
https://jcs.biologists.org/lookup/doi/10.1242/jcs.236497.supplemental

References

Babu, K., Cai, Y., Bahri, S., Yang, X. and Chia, W. (2004). Roles of Bifocal, Homer and F-actin in anchoring Oskar to the posterior cortex of Drosophila oocytes. *Genes Dev.* **18**, 138-143. doi:10.1101/gad.282604

Bachmann, A., Schneider, M., Theilenberg, E. Grawe, F. and Knust, E. (2001). Drosophila Stardust is a partner of Crumbs in the control of epithelial cell polarity. *Nature* **414**, 638-643. doi:10.1038/414638a

Barr, J., Yakovlev, K. V., Shidlovskii, Y. and Schedl, P. (2016). Establishing and maintaining cell polarity with mRNA localization in Drosophila. *BioEssays* **38**, 244-253. doi:10.1002/bies.201500088

Barrett, L. W., Fletcher, S. and Wilton, S. D. (2012). Regulation of eukaryotic gene expression by the untranslated gene regions and other non-coding elements. *Cell. Mol. Life Sci.* **69**, 3613-3634. doi:10.1007/s00018-012-0990-9

Bassett, A. and Liu, J.-L. (2014). CRISPR/Cas9 mediated genome engineering in Drosophila. *Methods* **69**, 128-136. doi:10.1016/j.ymeth.2014.02.019
Bergeman, J., Caillier, A., Houle, F., Gagné, L. M. and Huot, M.-É. (2016). Localized translation regulates cell adhesion and transendothelial migration. *J. Cell Sci.* **129**, 4105-4117. doi:10.1242/jcs.191320
Berger, S., Bulgakova, N. A., Grawe, F., Johnson, K. and Knust, E. (2007). Unraveling the genetic complexity of drosophila stardust during photoreceptor morphogenesis and prevention of light-induced degeneration. *Genetics* **176**, 2189-2200. doi:10.1534/genetics.107.071449
Bouvrette, L. P., Cody, N. A. L., Bergalet, J. Lefebvre, F. A. Diot, C. Wang, X. Blanchette, M. and Lécuyer, E. (2018). CeFra-seq reveals broad asymmetric mRNA and noncoding RNA distribution profiles in Drosophila and human cells. *RNA* **24**, 98-113. doi:10.1261/rna.063172.117
Brendza, R. P., Serbus, L. R., Duffy, J. B. and Saxton, W. M. (2000). A function for Kinesin I in the posterior transport of oskar mRNA and staufen protein. *Science* **289**, 2120-2122. doi:10.1126/science.289.5487.2120
Bulgakova, N. A. and Knust, E. (2009). The Crumbs complex: from epithelial-cell polarity to retinal degeneration. *J. Cell Sci.* **122**, 2587-2596. doi:10.1242/jcs.023648
Bullock, S. L. and Ish-Horowicz, D. (2001). Conserved signals and machinery for RNA transport in Drosophila oogenesis and embryogenesis. *Nature* **414**, 611-616. doi:10.1038/414611a
Bullock, S. L., Ringel, I., Ish-Horowicz, D. and Lukavsky, P. J. (2010). A′-form RNA helices are required for cytoplasmic mRNA transport in Drosophila. *Nat. Struct. Mol. Biol.* **17**, 703-709. doi:10.1038/nsmb.1813
Bullock, S. L., Stauber, M., Prell, A. Hughes, J. R. Ish-Horowicz, D. and Schmidt-Ott, U. (2004). Differential cytoplasmic mRNA localisation adjusts pair-rule transcription factor activity to cytoarchitecture in dipteran evolution. *Development* **131**, 4251-4261. doi:10.1242/dev.01289
Cao, H., Xu, R., Shi, Q., Zhang, D., Huang, J. and Hong, Y. (2017). FERM domain phosphorylation and endogenous 3′UTR are not essential for regulating the function and subcellular localization of polarity protein Crumbs. *J. Genet Genomics* **44**, 409-412. doi:10.1016/j.jgg.2017.08.002
Chartrand, P. M., Meng, X.-H., Singer, R. H. and Long, R. M. (1999). Structural elements required for the localization of ASH1 mRNA and of a green fluorescent protein reporter particle in vivo. *Curr. Biol.* **9**, 333-336. doi:10.1016/S0960-9822(99)80144-4
Clark, I., Giniger, E., Ruohola-Baker, H. Jan, L. Y. and Jan, Y. N. (1994). Transient posterior localization of a kinesin fusion protein reflects anteroposterior polarity of the Drosophila oocyte. *Curr. Biol.* **4**, 289-300. doi:10.1016/S0960-9822(00)00068-3
Cody, N. A., Iampietro, C. and Lécuyer, E. (2013). The many functions of mRNA localization during normal development and disease: from pillar to post. *Wiley Interdiscip Rev. Dev. Biol.* **2**, 781-796. doi:10.1002/wdev.113
Crucs, S., Chatterjee, S. and Gavis, E. R. (2000). Overlapping but distinct RNA elements control repression and activation of nanos translation. *Mol. Cell* **5**, 457-467. doi:10.1016/S1097-2765(00)80440-2
Cui, H., Ali, M. Y., Goyal, P., Zhang, K., Loh, J. Y., Trybus, K. M. and Solmaz, S. R. (2020). Coiled-coil registry shifts in the F684I mutant of Bicaudal D result in cargo-independent activation of dynein motility. *Traffic* **21**, 463-478. doi:10.1111/tra.12734
Davis, I. and Ish-Horowicz, D. (1991). Apical localization of pair-rule transcripts requires 3′ sequences and limits protein diffusion in the drosophila blastoderm embryo. *Cell* **67**, 927-940. doi:10.1016/0092-8674(91)90366-7
Delanoue, R. and Davis, I. (2005). Dynein anchors its mRNA cargo after apical transport in the Drosophila blastoderm embryo. *Cell* **122**, 97-106. doi:10.1016/j.cell.2005.04.033
Delanoue, R., Herpers, B., Soetaert, J., Davis, I. and Rabouille, C. (2007). Drosophila Squid/hnRNP helps Dynein switch from a gurken mRNA transport motor to an ultrastructural static anchor in sponge bodies. *Dev. Cell* **13**, 523-538. doi:10.1016/j.devcel.2007.08.022
Dienstbier, M., Boehl, F., Li, X. and Bullock, S. L. (2009). Egalitarian is a selective RNA-binding protein linking mRNA localization signals to the dynein motor. *Genes Dev.* **23**, 1546-1558. doi:10.1101/gad.531009
dos Santos, G., Simmonds, A. J. and Krause, H. M. (2008). A stem-loop structure in the wingless transcript defines a consensus motif for apical RNA transport. *Development* **135**, 133-143. doi:10.1242/dev.014068
Drosophila 12 Genomes Consortium, Clark, A. G., Eisen, M. B., Smith, D. R., Bergman, C. M., Oliver, B., Markow, T. A., Kaufman, T. C., Kellis, M., Gelbart, W. (2007). Evolution of genes and genomes on the Drosophila phylogeny. *Nature* **450**, 203-218. doi:10.1038/nature06341
Eritano, A. S., Altamirano, A., Beyeler, S., Gaytan, N., Velasquez, M., Riggs, B. and Marshall, W. (2017). The endoplasmic reticulum is partitioned asymmetrically during mitosis before cell fate selection in proneuronal cells in the early Drosophila embryo. *Mol. Biol. Cell* **28**, 1530-1538. doi:10.1091/mbc.e16-09-0690
Fletcher, G. C., Lucas, E. P., Brain, R., Tournier, A. and Thompson, B. J. (2012). Positive feedback and mutual antagonism combine to polarize crumbs in the drosophila follicle cell epithelium. *Curr. Biol.* **22**, 1116-1122. doi:10.1016/j.cub.2012.04.020
Flores-Benitez, D. and Knust, E. (2016). Dynamics of epithelial cell polarity in Drosophila: how to regulate the regulators? *Curr. Opin. Cell Biol.* **42**, 13-21. doi:10.1016/j.ceb.2016.03.018
Gavis, E. R. and Lehmann, R. (1994). Translational regulation of nanos by RNA localization. *Nature* **369**, 315-318. doi:10.1038/369315a0
Gavis, E. R., Curtis, D. and Lehmann, R. (1996). Identification of cis-acting sequences that control nanos RNA localization. *Dev. Biol.* **176**, 36-50. doi:10.1006/dbio.1996.9996
Goldman, C. H., Neiswender, H., Veeranan-Karmegam, R. and Gonsalvez, G. B. (2019). The Egalitarian binding partners Dynein light chain and Bicaudal-D act sequentially to link mRNA to the Dynein motor. *Development* **146**, dev176529. doi:10.1242/dev.176529
Grawe, F., Wodarz, A., Lee, B. Knust, E. and Skaer, H. (1996). The Drosophila genes crumbs and stardust are involved in the biogenesis of adherens junctions. *Development* **122**, 951-959.
Hamilton, R. S. and Davis, I. (2011). Identifying and searching for conserved RNA localisation signals. *Methods Mol. Biol.* **714**, 447-466. doi:10.1007/978-1-61779-005-8_27
Horne-Badovinac, S. and Bilder, D. (2008). Dynein regulates epithelial polarity and the apical localization of stardust A mRNA. *PLoS Genet.* **4**, 40-51.
Huang, J., Zhou, W., Dong, W., Watson, A. M. and Hong, Y. (2009). Directed, efficient and versatile modifications of the Drosophila genome by genomic engineering. *Proc. Natl. Acad. Sci. USA* **106**, 8284-8289. doi:10.1073/pnas.0900641106
Hughes, S. C. and Simmonds, A. J. (2019). Drosophila mRNA localization during later development: past, present, and future. *Front. Genet.* **10**, 135. doi:10.3389/fgene.2019.00135
Jambor, H., Surendranath, V., Kalinka, A. T., Mejstrik, P., Saalfeld, S. and Tomancak, P. (2015). Systematic imaging reveals features and changing localization of mRNAs in Drosophila development. *Elife* **4**, e05003. doi:10.7554/eLife.05003
Jansen, R.-P. and Niessing, D. (2012). Assembly of mRNA-protein complexes for directional mRNA transaport in eukaryotes-an overview. *Curr. Protein Pept. Sci.* **13**, 284-293. doi:10.2174/138920312801619493
Januschke, J. (2006). The centrosome-nucleus complex and microtubule organization in the Drosophila oocyte. *Development* **133**, 129-139. doi:10.1242/dev.02179
Kato, M., Han, T. W., Xie, S., Shi, K., Du, X., Wu, L. C., Mirzaei, H., Goldsmith, E. J., Longgood, J., Pei, J. et al. (2012). Cell-free formation of RNA granules: low complexity sequence domains form dynamic fibers within hydrogels. *Cell* **149**, 753-767. doi:10.1016/j.cell.2012.04.017
Kim-Ha, J. K., Kerr, K. and Macdonald, P. M. (1995). Translational regulation of oskar mRNA by bruno, an ovarian RNA-binding protein, is essential. *Cell* **81**, 403-412. doi:10.1016/0092-8674(95)90393-3
Knust, E., Dietrich, U., Tepass, U. Bremer, K. A. Wiegel, D. Vässin, H. and Campos-Ortega, J. A. (1987). EGF homologous sequences encoded in the genome of Drosophila melanogaster, and their relation to neurogenic genes. *EMBO J.* **6**, 761-766. doi:10.1002/j.1460-2075.1987.tb04818.x
Koch, E. A. and Spitzer, R. H. (1983). Multiple effects of Colchicine on oogenesis in Drosophila: Induced sterility and switch of potential oocyte to nurse-cell developmental pathway. *Cell Tissue Res.* **228**, 21-32. doi:10.1007/BF00206261
Kugler, J.-M. and Lasko, P. (2009). Localization, anchoring and translational control of oskar, gurken, bicoid and nanos mRNA during Drosophila oogenesis. *Fly (Austin)* **3**, 15-28. doi:10.4161/fly.3.1.7751
Kumichel, A., Kapp, K. and Knust, E. (2015). A conserved di-basic motif ofdrosophilacrumbs contributes to efficient ER export. *Traffic* **16**, 604-616. doi:10.1111/tra.12273
Laprise, P., Beronja, S., Silva-Gagliardi, N. F., Pellikka, M., Jensen, A. M., McGlade, C. J. and Tepass, U. (2006). The FERM protein yurt is a negative regulatory component of the crumbs complex that controls epithelial polarity and apical membrane size. *Dev. Cell* **11**, 363-374. doi:10.1016/j.devcel.2006.06.001
Larsen, K. S., Xu, J., Cermelli, S., Shu, Z. and Gross, S. P. (2008). BicaudalD actively regulates microtubule motor activity in lipid droplet transport. *PLoS ONE* **3**, e3763. doi:10.1371/journal.pone.0003763
Lasko, P. (2011). Posttranscriptional regulation in Drosophilaoocytes and early embryos. *RNA* **2**, 408-416. doi:10.1002/wrna.70
Lasko, P. (2012). mRNA localization and translational control in Drosophila oogenesis. *Cold Spring Harb. Perspect Biol.* **4**, a012294. doi:10.1101/cshperspect.a012294
Lazzaretti, D. and Bono, F. (2017). mRNA localization in metazoans: a structural perspective. *RNA Biol.* **14**, 1473-1484. doi:10.1080/15476286.2017.1338231
Le Bivic, A. (2013). Evolution and cell physiology. 4. Why invent yet another protein complex to build junctions in epithelial cells? *Am. J. Physiol. Cell Physiol.* **305**, C1193-C1201. doi:10.1152/ajpcell.00272.2013
Lécuyer, E., Yoshida, H., Parthasarathy, N., Alm, C., Babak, T., Cerovina, T., Hughes, T. R., Tomancak, P. and Krause, H. M. (2007). Global analysis of mRNA localization reveals a prominent role in organizing cellular architecture and function. *Cell* **131**, 174-187. doi:10.1016/j.cell.2007.08.003

Li, Z., Wang, L., Hays, T. S. and Cai, Y. (2008). Dynein-mediated apical localization ofcrumbstranscripts is required for Crumbs activity in epithelial polarity. *J. Cell Biol.* **180**, 31-38. doi:10.1083/jcb.200707007

Liu, Y., Salter, H. K., Holding, A. N., Johnson, C. M., Stephens, E., Lukavsky, P. J., Walshaw, J. and Bullock, S. L. (2013). Bicaudal-D uses a parallel, homodimeric coiled coil with heterotypic registry to coordinate recruitment of cargos to dynein. *Genes Dev.* **27**, 1233-1246. doi:10.1101/gad.212381.112

Macara, I. G., Guyer, R., Richardson, G., Huo, Y. and Ahmed, S. M. (2014). Epithelial homeostasis. *Curr. Biol.* **24**, R815-R825. doi:10.1016/j.cub.2014.06.068

Macdonald, P. M., Kerr, K., Smith, J. L. and Leask, A. (1993). RNA regulatory element BLE1 directs the early steps of bicoid mRNA localization. *Development* **118**, 1233-1243.

Mach, J. M. and Lehmann, R. (1997). An egalitarian-BicaudalD complex is essential for oocyte specification and axis determination in Drosophila. *Genes Dev.* **11**, 423-435. doi:10.1101/gad.11.4.423

Mayr, C. (2017). Regulation by 3′-untranslated regions. *Annu. Rev. Genet.* **51**, 171-194. doi:10.1146/annurev-genet-120116-024704

McNeil, G. P., Kaur, M., Purrier, S. and Kang, R. (2009). The Drosophila RNA-binding protein Lark is required for localization of Dmoesin to the oocyte cortex during oogenesis. *Dev. Genes Evol.* **219**, 11-19. doi:10.1007/s00427-008-0260-x

Medioni, C., Mowry, K. and Besse, F. (2012). Principles and roles of mRNA localization in animal development. *Development* **139**, 3263-3276. doi:10.1242/dev.078626

Mohler, J. Y. M. and Wieschaus, E. F. (1986). Dominant maternal effect mutations of Drosophila melanogaster causing the production of double abdomen embryos. *Genetics* **112**, 803-822.

Moor, A. E., Golan, M., Massasa, E. E. Lemze, D. Weizman, T. Shenhav, R. Baydatch, S. Mizrahi, O. Winkler, R. Golani, R.et al. (2017). Global mRNA polarization regulates translation efficiency in the intestinal epithelium. *Science* **357**, 1299-1303. doi:10.1126/science.aan2399

Muschalik, N. and Knust, E. (2011). Increased levels of the cytoplasmic domain of Crumbs repolarise developing Drosophila photoreceptors. *J. Cell Sci.* **124**, 3715-3725. doi:10.1242/jcs.091223

Nakamura, A., Amikura, R., Hanyu, K. and Kobayashi, S. (2001). Me31B silences translation of oocyte-localizing RNAs through the formation of cytoplasmic RNP complex during Drosophila oogenesis. *Development* **128**, 3233-3242.

Navarro, C., Puthalakath, H., Adams, J. M., Strasser, A. and Lehmann, R. (2004). Egalitarian binds dynein light chain to establish oocyte polarity and maintain oocyte fate. *Nat. Cell Biol.* **6**, 427-435. doi:10.1038/ncb1122

Parton, R. M., Davidson, A., Davis, I. and Weil, T. T. (2014). Subcellular mRNA localisation at a glance. *J. Cell Sci.* **127**, 2127-2133. doi:10.1242/jcs.114272

Pellikka, M., Tanentzapf, G., Pinto, M., Smith, C., McGlade, C. J., Ready, D. F. and Tepass, U. (2002). Crumbs, the Drosophila homologue of human CRB1/RP12, is essential for photoreceptor morphogenesis. *Nature* **416**, 143-149. doi:10.1038/nature721

Perez-Mockus, G., Mazouni, K., Roca, V., Corradi, G., Conte, V. and Schweisguth, F. (2017). Spatial regulation of contractility by Neuralized and Bearded during furrow invagination in Drosophila. *Nat. Commun.* **8**, 1594. doi:10.1038/s41467-017-01482-8

Port, F., Chen, H.-M., Lee, T. and Bullock, S. L. (2014). Optimized CRISPR/Cas tools for efficient germline and somatic genome engineering in Drosophila. *Proc. Natl Acad. Sci. USA* **111**, E2967-E2976. doi:10.1073/pnas.1405500111

Richard, M., Grawe, F. and Knust, E. (2006). DPATJ plays a role in retinal morphogenesis and protects against light-dependent degeneration of photoreceptor cells in the Drosophila eye. *Dev. Dyn.* **235**, 895-907. doi:10.1002/dvdy.20595

Rodriguez-Boulan, E. and Macara, I. G. (2014). Organization and execution of the epithelial polarity programme. *Nat. Rev. Mol. Cell Biol.* **15**, 225-242. doi:10.1038/nrm3775

Ryder, P. V. and Lerit, D. A. (2018). RNA localization regulates diverse and dynamic cellular processes. *Traffic* **19**, 496-502. doi:10.1111/tra.12571

Ryu, Y. H., Kenny, A., Gim, Y., Snee, M. and Macdonald, P. M. (2017). Multiplecis-acting signals, some weak by necessity, collectively direct robust transport ofoskarmRNA to the oocyte. *J. Cell Sci.* **130**, 3060-3071. doi:10.1242/jcs.202069

Schindelin, J., Arganda-Carreras, I., Frise, E., Kaynig, V., Longair, M., Pietzsch, T., Preibisch, S., Rueden, C., Saalfeld, S., Schmid, B. et al. (2012). Fiji: an open-source platform for biological-image analysis. *Nat. Meth.* **9**, 676-682. doi:10.1038/nmeth.2019

Schroeder, S. J. (2018). Challenges and approaches to predicting RNA with multiple functional structures. *RNA* **24**, rna.067827.067118. doi:10.1261/rna.067827.118

Schüpbach, T. and Wieschaus, E. F. (1991). Female sterile mutations on the second chromosome of Drosophila melanogaster. II. Mutations blocking oogenesis or altering egg morphology. *Genetics* **129**, 1119-1136.

Sebo, Z. L., Lee, H. B., Peng, Y. and Guo, Y. (2014). A simplified and efficient germline-specific CRISPR/Cas9 system for Drosophila genomic engineering. *Fly (Austin)* **8**, 52-57. doi:10.4161/fly.26828

Sherrard, K. M. and Fehon, R. G. (2015). The transmembrane protein Crumbs displays complex dynamics during follicular morphogenesis and is regulated competitively by Moesin and aPKC. *Development* **142**, 2226-2226. doi:10.1242/dev.126425

Simmonds, A. J., dosSantos, G., Livne-Bar, I. and Krause, H. M. (2001). Apical localization of wingless transcripts is required for Wingless signalling. *Cell* **105**, 197-207. doi:10.1016/S0092-8674(01)00311-7

Suyama, R., Jenny, A., Curado, S., Pellis-van Berkel, W. and Ephrussi, A. (2009). The actin-binding protein Lasp promotes Oskar accumulation at the posterior pole of the Drosophila embryo. *Development* **136**, 95-105. doi:10.1242/dev.027698

Tanentzapf, G., Smith, C., McGlade, J. and Tepass, U. (2000). Apical, lateral, and basal polarization cues contribute to the development of the follicular epithelium during Drosophila oogenesis. *J. Cell Biol.* **151**, 891-904. doi:10.1083/jcb.151.4.891

Tepass, U. (1996). Crumbs, a component of the apical membrane, is required for zonulas adhrens formation in primary epithelia of Drosophila. *Dev. Biol.* **177**, 217-225. doi:10.1006/dbio.1996.0157

Tepass, U. (2012). The apical polarity protein network in drosophila epithelial cells: regulation of polarity, junctions, morphogenesis, cell growth, and survival. *Annu. Rev. Cell Dev. Biol.* **28**, 655-685. doi:10.1146/annurev-cellbio-092910-154033

Tepass, U. and Knust, E. (1990). Phenotypic and developmental analysis of mutations at the crumbs locus, a gene requried for the development of epithelia in Drosophila melanogaster. *Roux's Arch Dev. Biol.* **199**, 189-206. doi:10.1007/BF01682078

Tepass, U., Theres, C. and Knust, E. (1990). crumbs encodes an EGF-like protein expressed on apical membranes of Drosophila epithelia cells and required for organization of epithelia. *Cell* **61**, 787-799. doi:10.1016/0092-8674(90)90189-L

Theurkauf, W. E., Smiley, S., Wong, M. L. and Alberts, B. M. (1992). Reorganisation of the cytoskeleton during Drosophila oogenesis: implications for axis specification and intercellular transport. *Development* **115**, 923-936.

Tomancak, P., Beaton, A., Weiszmann, R., Kwan, E., Shu, S. Q., Lewis, S. E., Richards, S., Ashburner, M., Hartenstein, V., Celniker, S. E. et al. (2002). Systematic determination of patterns of gene expression during Drosophila embryogenesis. *Genome Biol.* **3**, research0088.1. doi:10.1186/gb-2002-3-12-research0088

Van De Bor, V., Zimniak, G., Cérézo, D., Schaub, S. and Noselli, S. (2011). Asymmetric localisation of cytokine mRNA is essential for JAK/STAT activation during cell invasiveness. *Development* **138**, 1383-1393. doi:10.1242/dev.056184

Vazquez-Pianzola, P. and Suter, B. (2012). Conservation of the RNA transport machineries and their coupling to translation control across eukaryotes. *Comp. Funct. Genom.* **2012**, 1-13. doi:10.1155/2012/287852

Vazquez-Pianzola, P., Adam, J., Haldemann, D., Hain, D., Urlaub, H. and Suter, B. (2014). Clathrin heavy chain plays multiple roles in polarizing the Drosophila oocyte downstream of Bic-D. *Development* **141**, 1915-1926. doi:10.1242/dev.099432

Vazquez-Pianzola, P., Schaller, B., Colombo, M., Beuchle, D., Neuenschwander, S., Marcil, A., Bruggmann, R. and Suter, B. (2017). The mRNA transportome of the BicD/Egl transport machinery. *RNA Biol.* **14**, 73-89. doi:10.1080/15476286.2016.1251542

Weil, T. T. (2014). mRNA localization in the Drosophila germline. *RNA Biol.* **11**, 1010-1018. doi:10.4161/rna.36097

Weil, T. T., Forrest, K. M. and Gavis, E. R. (2006). Localization of bicoid mRNA in late oocytes is maintained by continual active transport. *Dev. Cell* **11**, 251-262. doi:10.1016/j.devcel.2006.06.006

Weis, B. L., Schleiff, E. and Zerges, W. (2013). Protein targeting to subcellular organelles via MRNA localization. *Biochim. Biophys. Acta* **1833**, 260-273. doi:10.1016/j.bbamcr.2012.04.004

Wieschaus, E. F. and Nüsslein-Volhard, C. (1986). Looking at embryos. In *Drosophila, a Practical Approach* (ed. D. B. Roberts), pp. 199-227. Oxford: IRL Press.

Wilk, R., Hu, J., Blotsky, D. and Karause, H. M. (2016). Diverse and pervasive subcellular distributions for both voding and long noncoding RNAs. *Genes Dev.* **30**, 594-609. doi:10.1101/gad.276931.115

Wilkie, G. S. and Davis, I. (2001). Drosophila wingless and Pair-Rule transcripts localize apically by Dynein-mediated transport of RNA particles. *Cell* **105**, 209-219. doi:10.1016/S0092-8674(01)00312-9

Wodarz, A., Hinz, U., Engelbert, M. and Knust, E. (1995). Expression of Crumbs confers apical character on plasma membrane domains of ectodermal epithelia of Drosophila. *Cell* **82**, 67-76. doi:10.1016/0092-8674(95)90053-5

Zuker, M. (2003). Mfold web server for nucleic acid folding and hybridization prediction. *Nucleic Acids Res.* **31**, 3406-3415. doi:10.1093/nar/gkg595